TRIUMF

CANADA'S NATIONAL LABORATORY FOR PARTICLE AND NUCLEAR PHYSICS

Owned and operated as a joint venture by a consortium of Canadian universities via a contribution through the National Research Council Canada

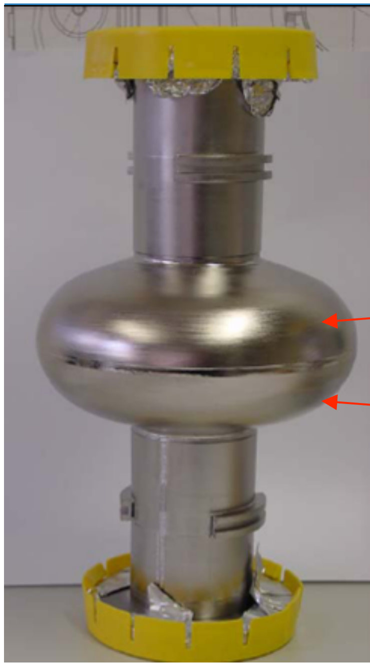

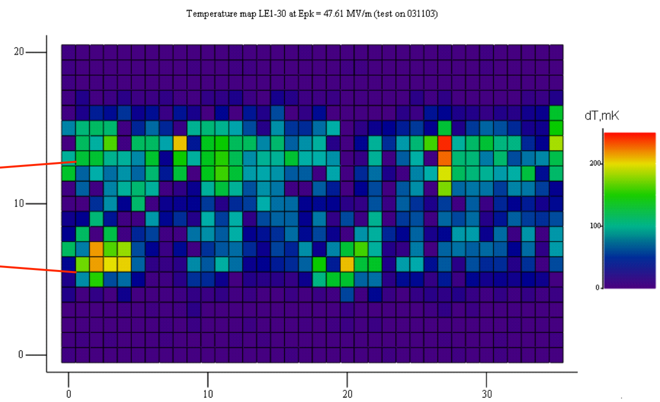

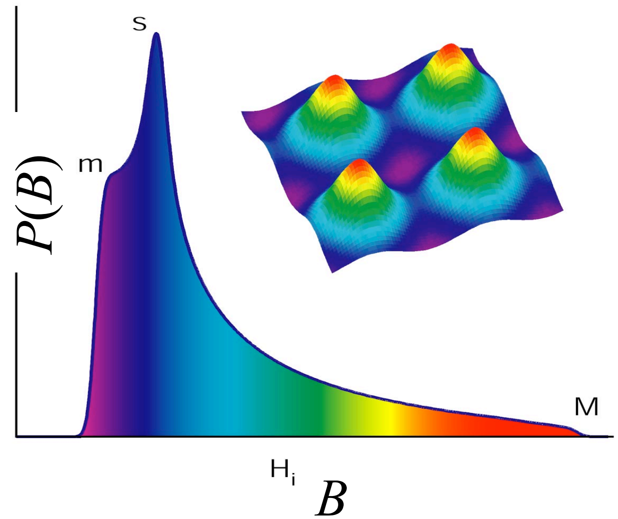

Muon Spin Rotation/Relaxation Studies of Niobium for SRF Applications

Anna Grassellino, Ph.D. Candidate, University of Pennsylvania

LABORATOIRE NATIONAL CANADIEN POUR LA RECHERCHE EN PHYSIQUE NUCLÉAIRE ET EN PHYSIQUE DES PARTICULES

Propriété d'un consortium d'universités canadiennes, géré en co-entreprise à partir d'une contribution administrée par le Conseil national de recherches Canada

Superconductivity

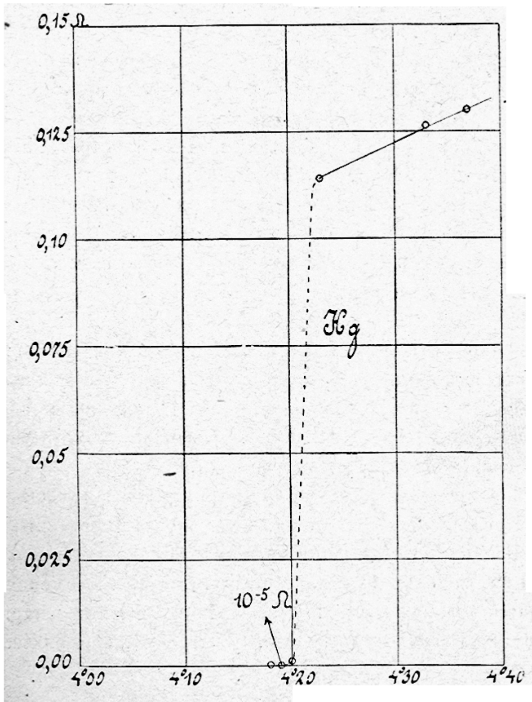

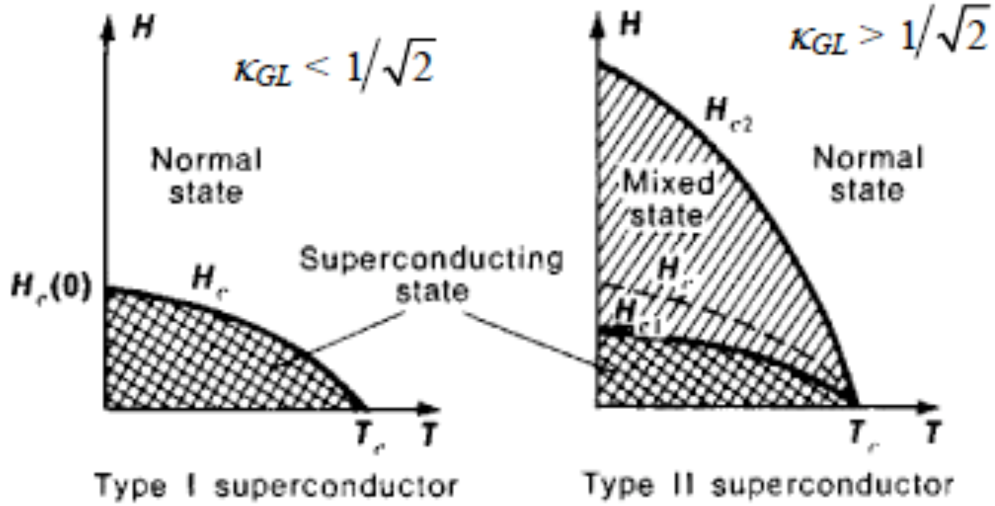

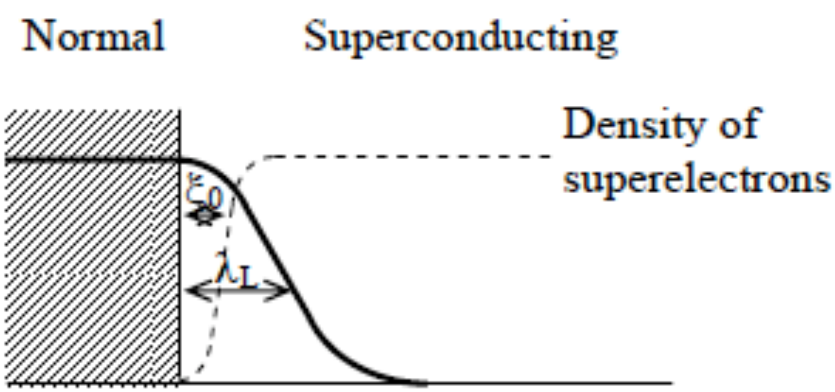

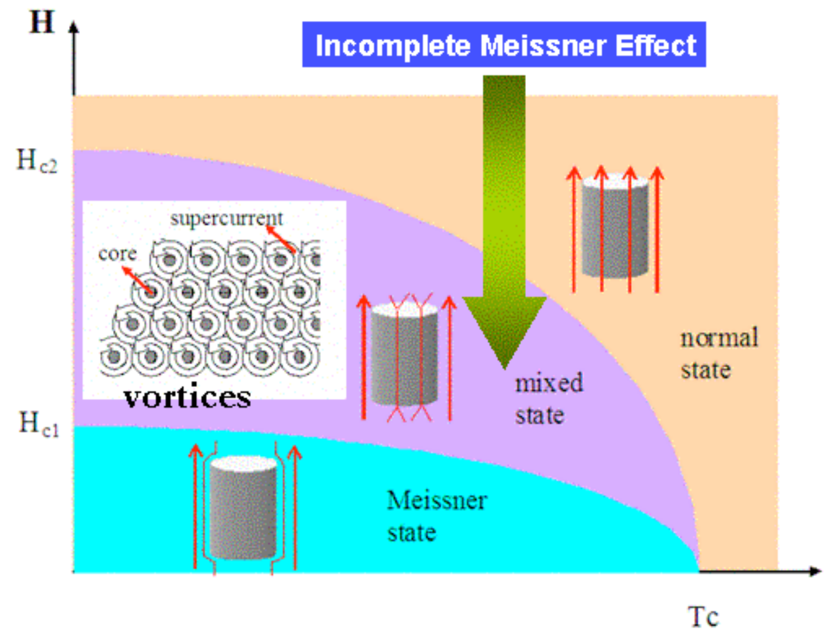

Q-slopes in Nb cavities

- Degradation of quality factor with the applied RF field
- Medium field Q-slope: gradual decrease in range Hpk~20-100 mT
- High field Q-drop: sharp losses above peak field ~80-100 mT
- 120C bake 48 hrs UHV improves/removes HFQS

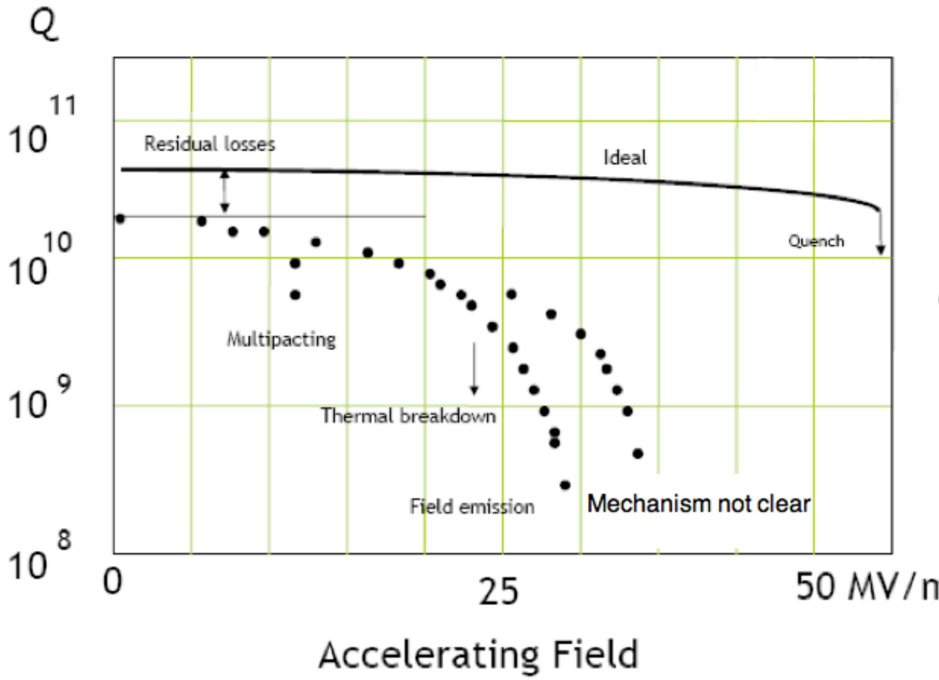

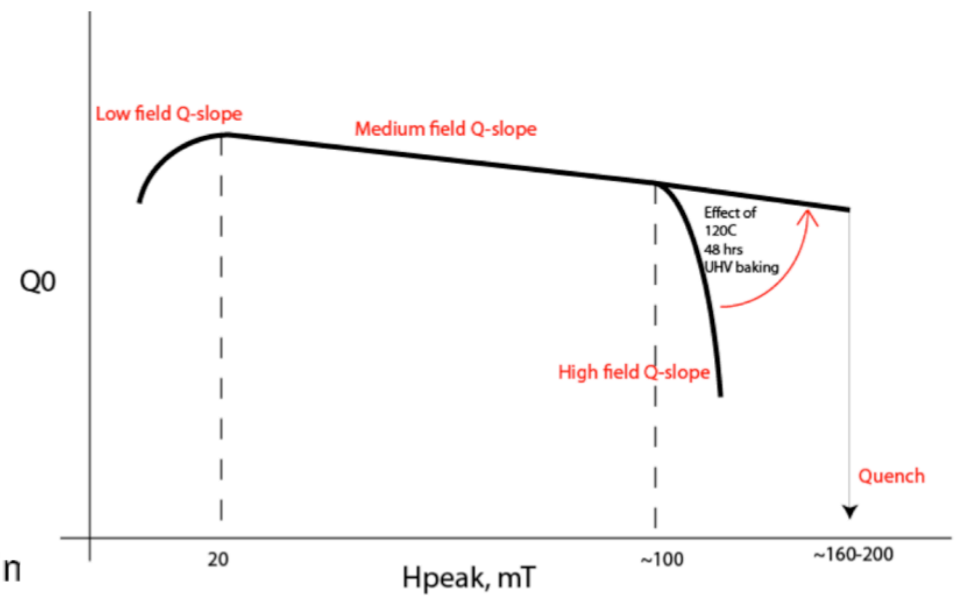

- Huge number of models in the history of SRF to explain Q-slopes
- <u>None so far unconfutably proves causes or mechanisms</u>

TRIUMF

Models for HFQS

Theories / Experiments Confrontation

B. Visentin - SRF (2003) – updated at Argonne Workshop (2004)

	Q-Slope Fit	Q-Slope before baking (EP = BCP)	Q-Slope Improvem't after baking	Q-Slope after baking (EP < BCP)	No change after 4 y. air exposure	Exceptional Results (BCP)	Q-Slope unchanged after HF chemistry	TE_{011} Q-slope after baking	Quench EP > BCP	BCP Quench unchanged after baking	Argum't Validity	Fund'al Disagreem't Exper. ≠ Theory
Magnetic Field Enhancem't	**Y** simulat. code	~~**N**~~ $\beta_m \neq B_{C2}^S \neq$	**Y** $B_{C2}^S \uparrow$	**Y** lower β_m	-	**N** high β_m	-	-	**Y** lower β_m	**N** $B_{C2}^S \uparrow$	**Y**	**D_1**
Interface Tunnel Exchange	**Y** E^s	**N** $\beta^* \neq$	**Y** $Nb_2O_{5-y} \downarrow$	**Y** lower β^*	**N** $Nb_2O_{5-y} \uparrow$	**N** high β^*	~~**N**~~ new Nb_2O_{5-y}	~~**N**~~ improv't	-	-	**Y**	**D_2**
Thermal Feedback	**Y** parabolic	**Y** ≅ thermal properties	**Y** $R_{BCS}\downarrow$ $R_{res}\uparrow$	**N** ≅ therm. propties	-	-	-	-	-	-	**N** C coeff't	-
Magnetic Field Dependence of Δ	**Y** expon'tial	**N** $B_{C2}^S \neq$	**Y** $B_{C2}^S \uparrow$	**Y** higher B_{C2}^S	-	-	-	-	-	-	~~**N**~~ thin film	**D_1**
Segregation of Impurities	?	**N** segregation ≠	**N** only O diffusion	**Y** surface ≠	-	**Y** good cleaning	**N** chemistry	-	-	-	**Y**	-
Bad S.C. Layer Interstitial Oxygen $Nb_{4-6}O$	?	**Y** NC layer	**Y** O diffusion	**N**	**N** interstitial re-appears	-	~~**N**~~ new bad layer	-	**Y** higher B_{C2}^S	**N** $B_{C2}\downarrow$	**Y**	**D_1**

Y / **N** = theory in **agreement** / **contradiction** with experimental observation **N+**

/ = undisputable disagreement with experiment

HFQS: early flux penetration?

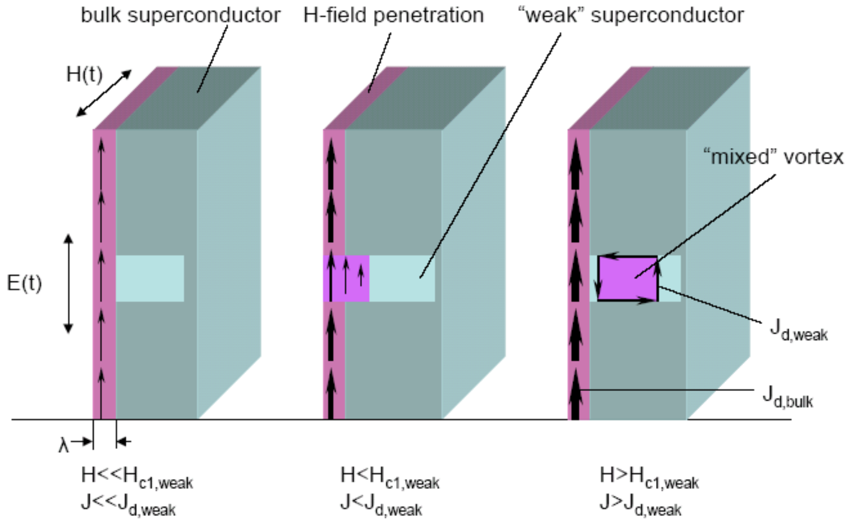

P.Bauer, Review of Q-drop models

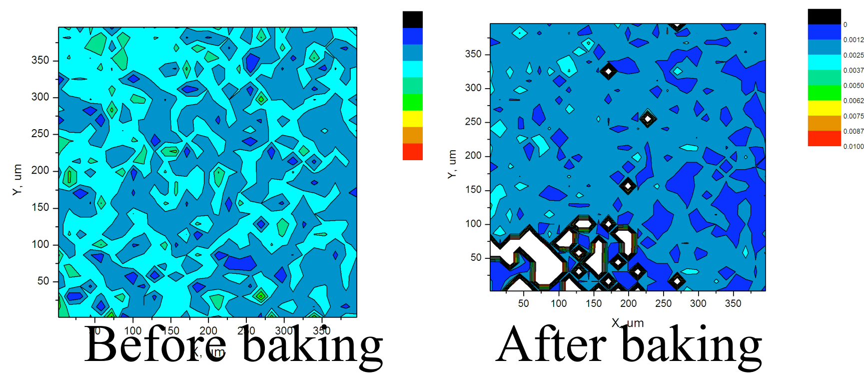

[A Romanenko and H Padamsee 2010 *Supercond. Sci. Technol.* ***23 045008***]

•'Weaker' superconducting regions allow 'premature' magnetic flux entry

•Cutout samples studies: decrease in average dislocation density observed by EBSD after 120C baking (which removes the HFQS in cavities)

•<u>Working hypothesis</u> – surface dislocations provide sites for early flux penetration (below bulk Hc1)

HFQS: early flux penetration?

- **GOAL: Design an experiment to prove magnetic flux entry as the right or wrong <u>mechanism</u> behind HFQS**
- Study field of flux entry (and other superconducting properties) in **HFQS limited cutout samples**:
  - Hot vs cold
  - **Baked vs unbaked**
- Need of local, sensitive magnetic field probe: Muon Spin Rotation
- First time in SRF we attempt to measure superconducting parameters of Nb cut out of cavities with muSR

Cutout samples: large grain, small grain BCP

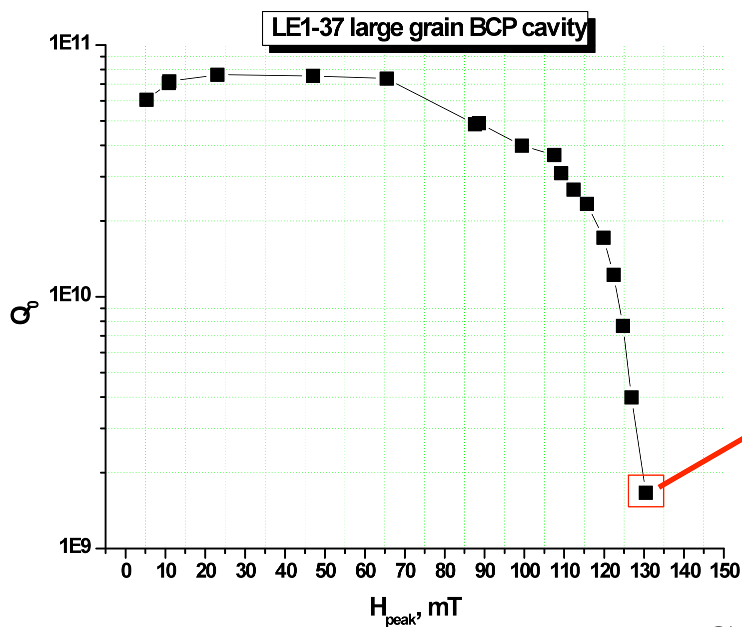

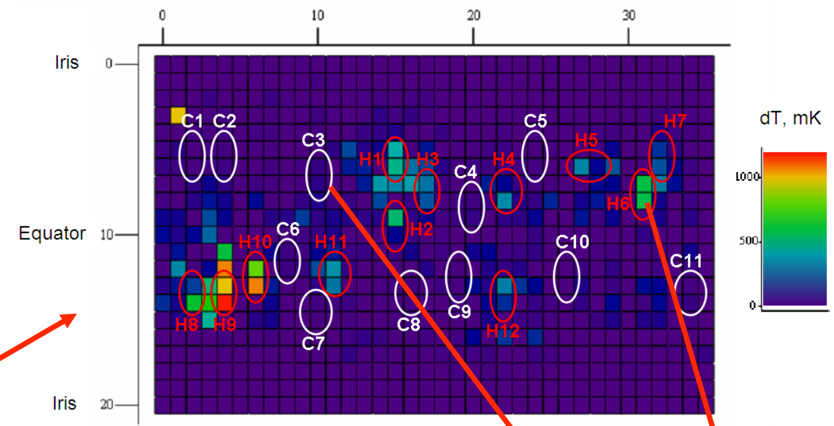

RF Side

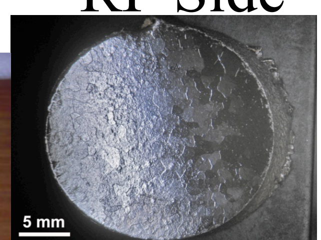

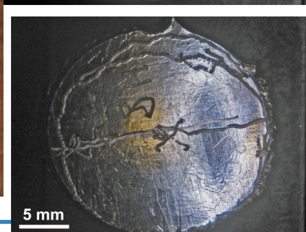

Outer Side

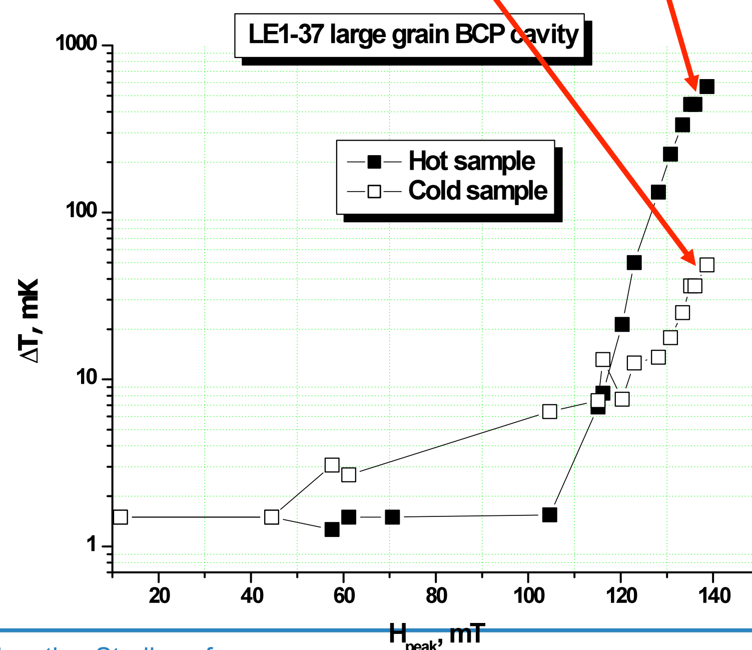

A. Romanenko Ph.D. thesis

RF characterization of samples studied (A.Romanenko)

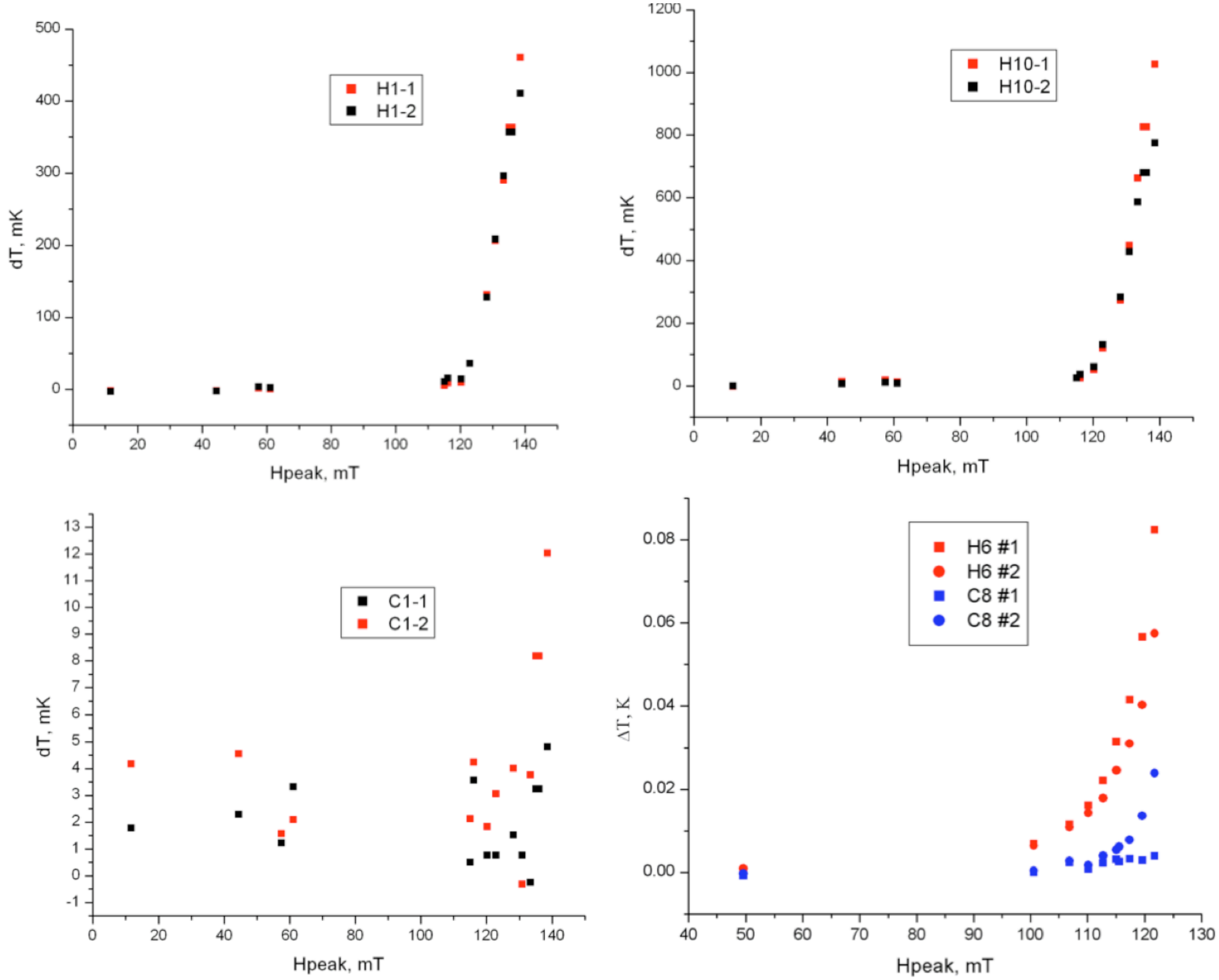

LOCAL probe of magnetism: muSR

	Conventional Methods		Nuclear Beam Methods	
	NMR	ESR	μSR	β-NMR
Probe:	host nuclei	host electrons	muons	radioactive nuclei
Lifetime:	infinite	infinite	2.2 μs	100 ms - hours
Polarization Method:	apply large field	apply large field	natural	optical pumping
Polarization (max.):	<< 1 %	<< 1 %	100 %	80 %
Detection:	absorbed RF radiation	absorbed microwave radiation	anisotropic decay of muon	anisotropic decay of nucleus
Sensitivity:	10^{17} spins	10^{17} spins	10^{7} spins	10^{7} spins

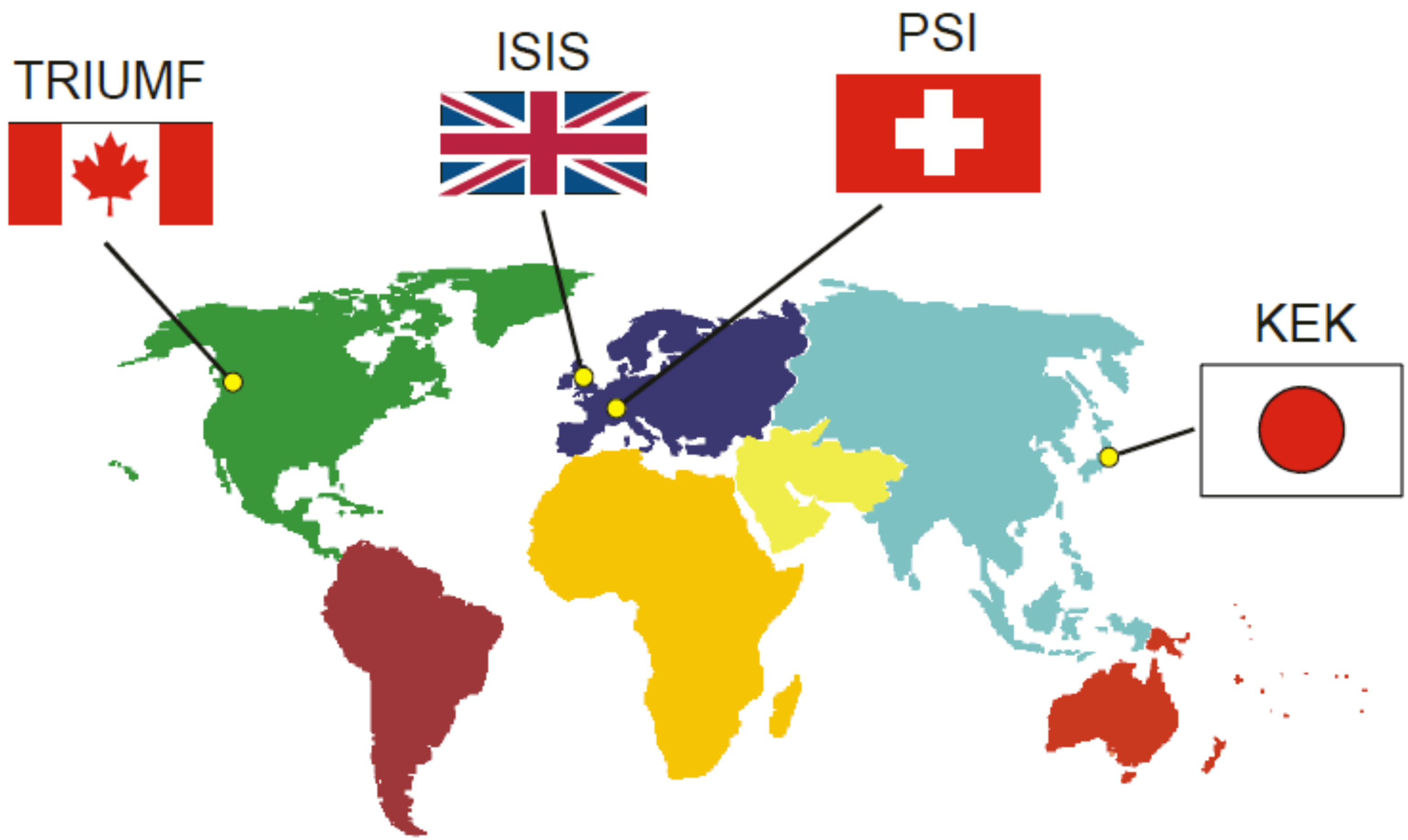

μSR facilities of the world.

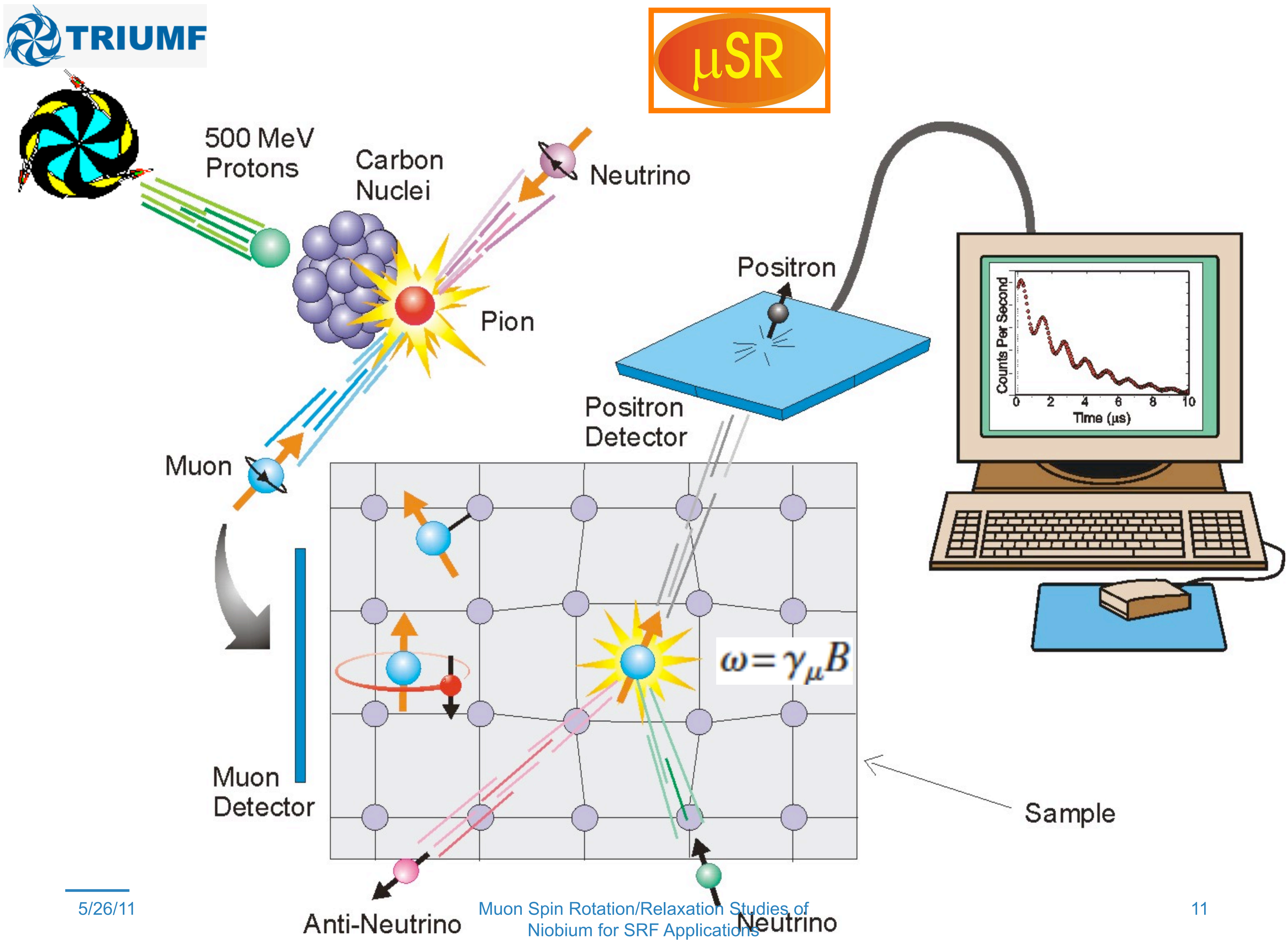
TRIUMF
μSR
500 MeV
Protons
Carbon
Nuclei
Neutrino
Pion
Positron
Positron
Detector
Counts Per Second
Time (μs)
0
2
4
6
8
10
Muon
$\omega = \gamma_\mu B$
Muon
Detector
Sample
Anti-Neutrino
Neutrino

Pion Decay: $\pi^+ \rightarrow \mu^+ + \nu_\mu$

A pion resting on the downstream side of the primary production target has zero linear momentum and zero angular momentum.

Conservation of Linear Momentum: μ^+ emitted with momentum equal and opposite to that of the ν_μ

Conservation of Angular Momentum: μ^+ and the ν_μ have equal and opposite spin

Weak Interaction: only "left-handed" ν_μ are created. **Therefore the emerging μ^+ has its spin pointing antiparallel to its momentum direction**

→ 100% spin polarized!

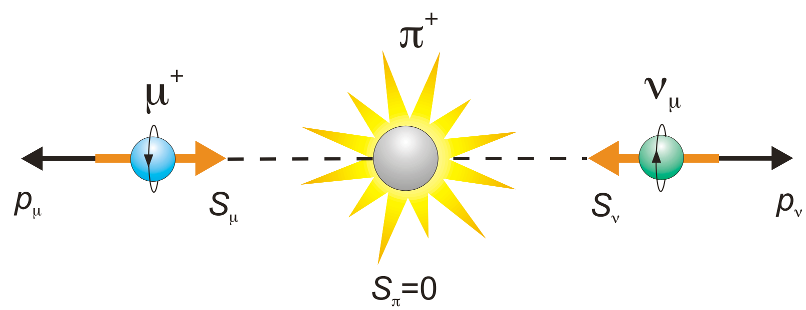

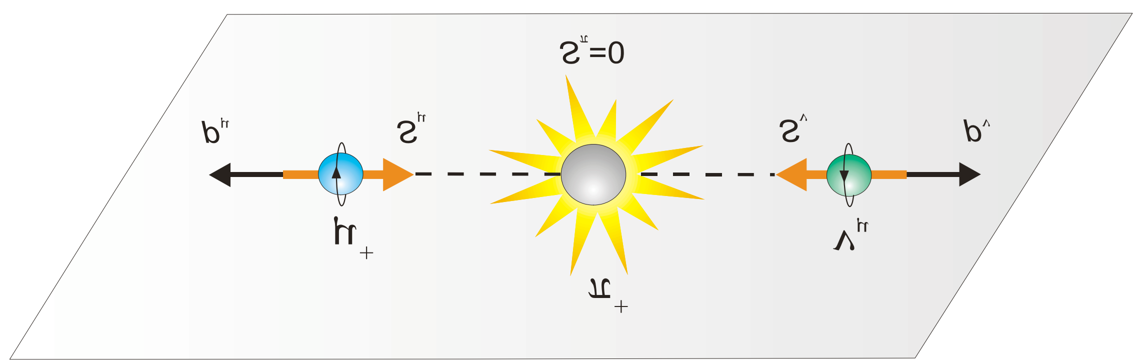

μ^+-Decay Asymmetry

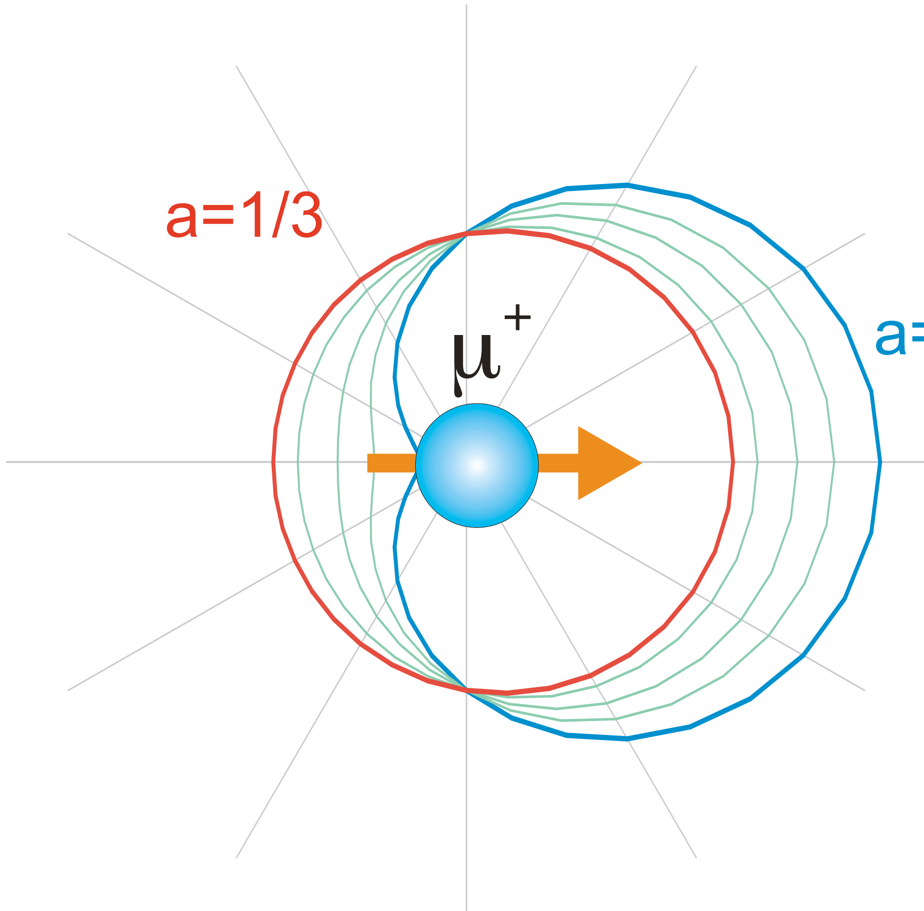

$$\mu^+ \rightarrow e^+ + \nu_e + \overline{\nu}_\mu$$

$$\mu^- \rightarrow e^- + \overline{\nu}_e + \nu_\mu$$

Angular distribution of positrons from the μ^+-decay. The asymmetry is a = 1/3 when all positron energies are sampled with equal probability.

The muon is sensitive to the **vector sum** of the local magnetic fields at its stopping site. The local fields consist of:

- those from **nuclear** magnetic moments
- those from **electronic** moments (100-1000 times larger than from nuclear moments)
- **external** magnetic fields

As a local probe, μSR can be used to deduce Magnetic volume fractions.

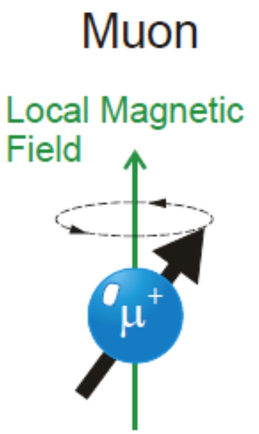

$$\omega = \gamma_\mu B$$

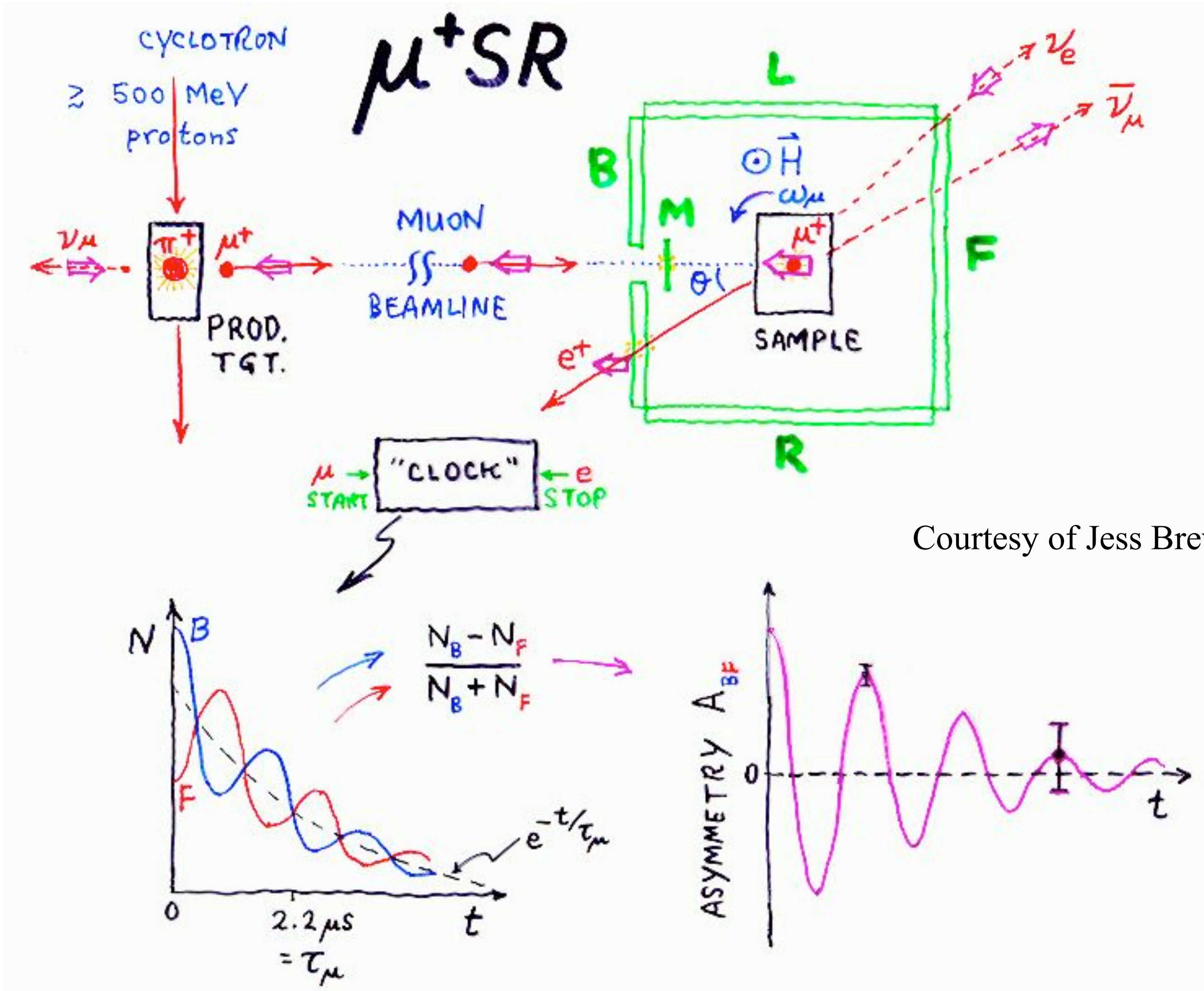

Courtesy of Jess Brewer, TRIUMF

Transverse-Field μSR: vortex lattice studies, measurement of λ, ξ, G-L parameter k

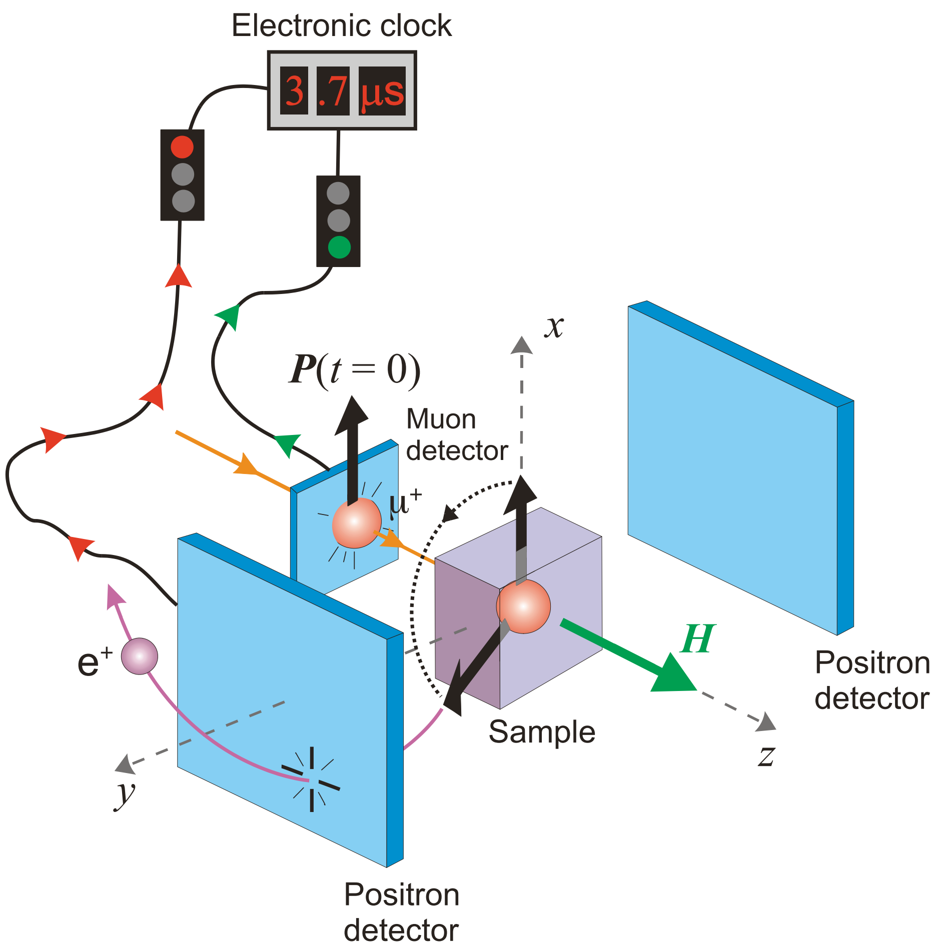

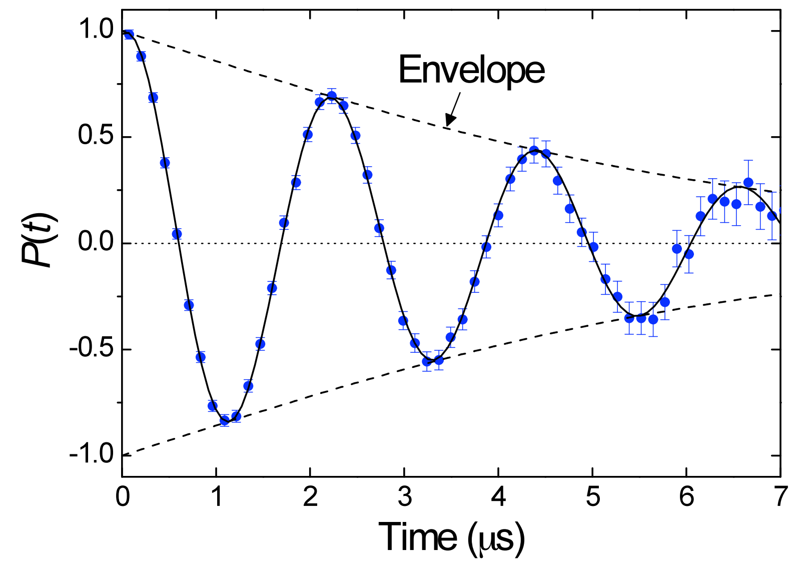

The time evolution of the muon spin polarization is described by:

$$P(t) = G(t)\cos(\gamma_{\mu} B_{\mu} t + \phi)$$

where $G(t)$ is a relaxation function describing the ***envelope*** of the TF-μSR signal that is sensitive to the width of the static field distribution or temporal fluctuations.

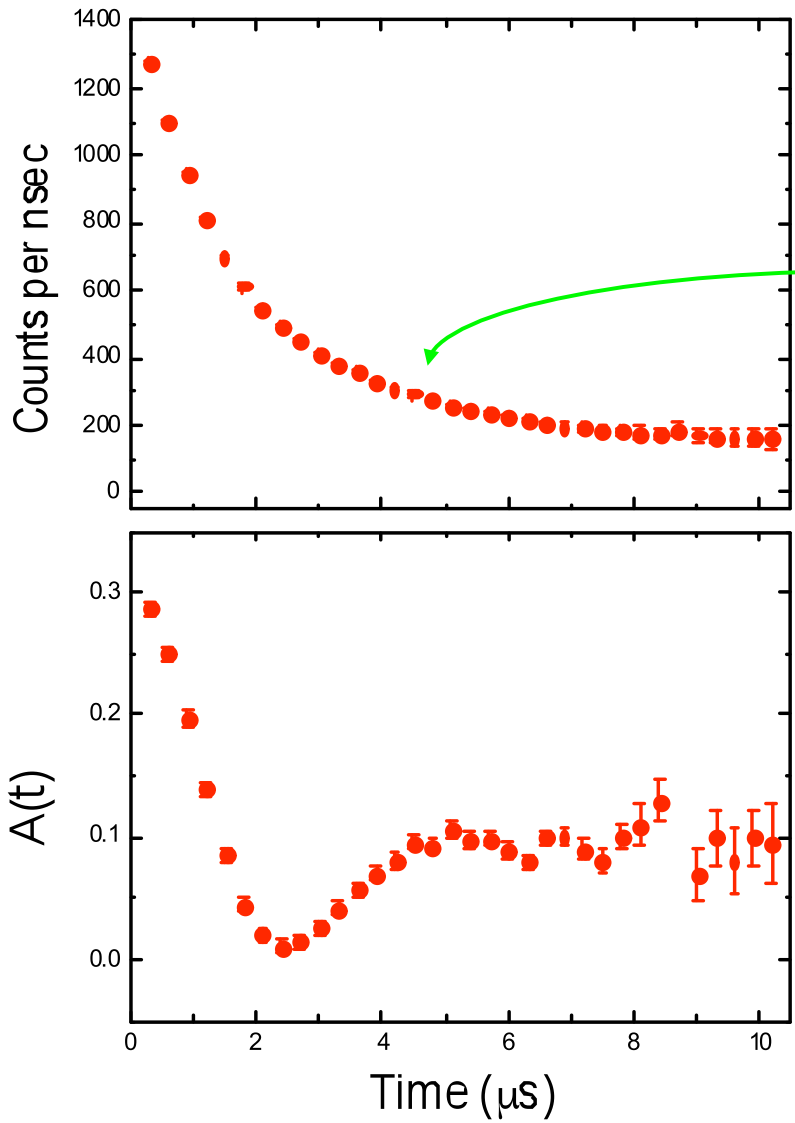

The **count rates** for opposing e^+ detectors:

$$N_B(t) = N_0 e^{-t/\tau_\mu}\left[1 + a_0 G(t)\cos(\gamma_\mu B_\mu t + \Phi)\right]$$

$$N_F(t) = N_0 e^{-t/\tau_\mu}\left[1 - a_0 G(t)\cos(\gamma_\mu B_\mu t + \Phi)\right]$$

Forming the *B-F* count rate ratio:

$$\frac{N_B(t) - N_F(t)}{N_B(t) + N_F(t)} = a_0 G(t)\cos(\gamma_\mu B_\mu t + \Phi)$$

$$= a_0 P(t) \equiv A(t)$$

μSR asymmetry spectrum

Zero-Field μSR: internal field distribution, magnetic impurities, trapped flux

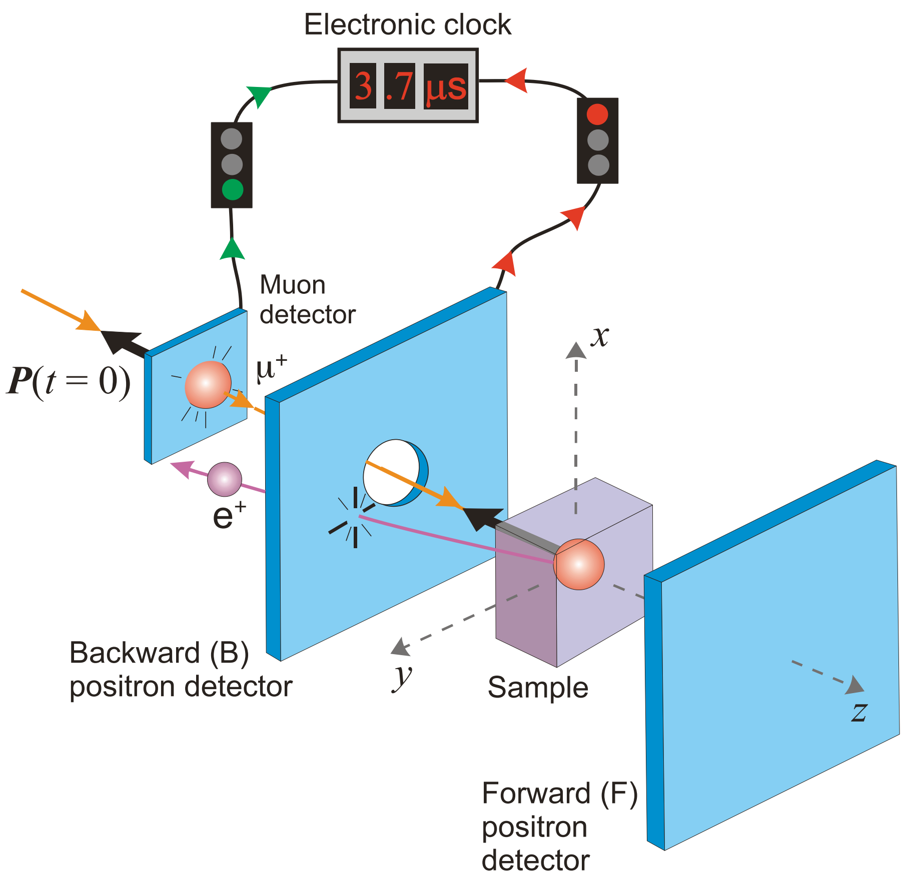

The **count rates** for opposing e^+ detectors:

$$N_B(t) = N_0 e^{-t/\tau_\mu}\left[1 + a_0 G(t)\cos(\gamma_\mu B_\mu t + \Phi)\right]$$

$$N_F(t) = N_0 e^{-t/\tau_\mu}\left[1 - a_0 G(t)\cos(\gamma_\mu B_\mu t + \Phi)\right]$$

The corresponding μ^+ spin relaxation function is known as the ***Kubo-Toyabe function***

$$G_z(t) = \frac{1}{3} + \frac{2}{3}\left(1 - \Delta^2 t^2\right)\exp\left(-\frac{1}{2}\Delta^2 t^2\right)$$

Magnetic field distribution of a vortex lattice

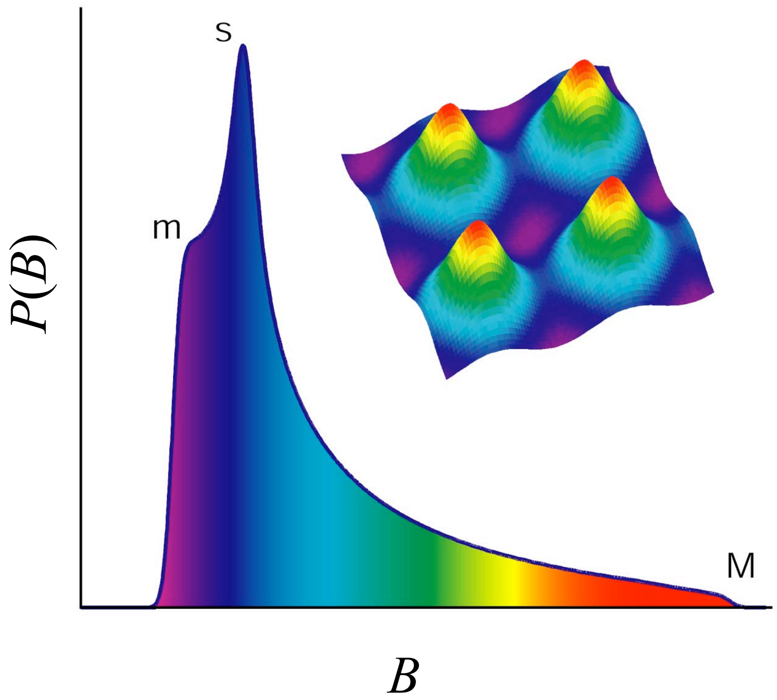

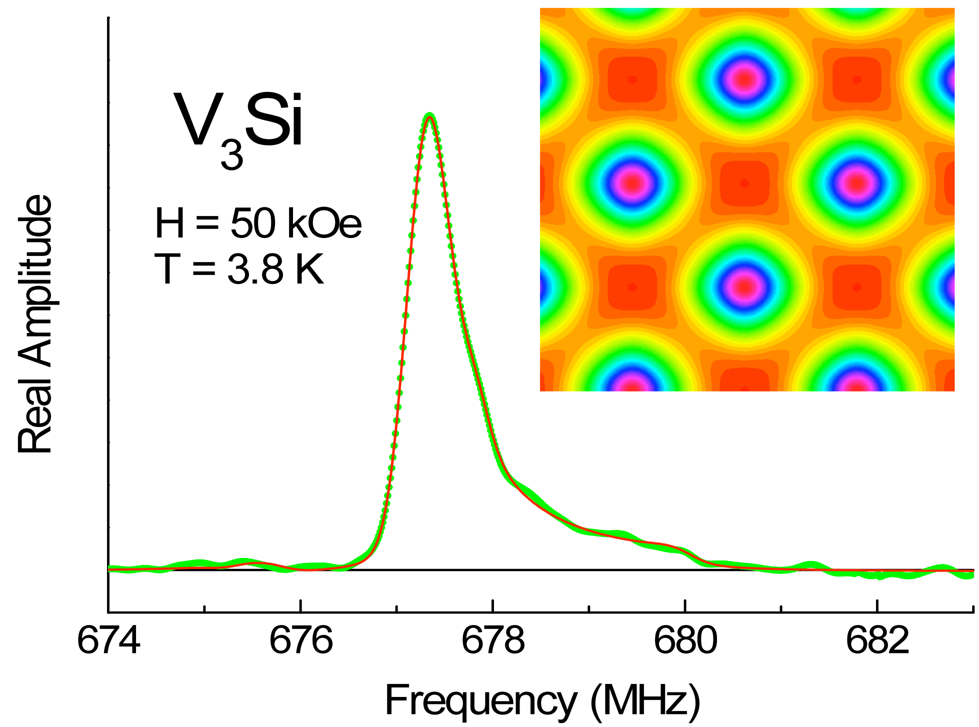

Asymmetry spectrum plotted in a rotating reference frame

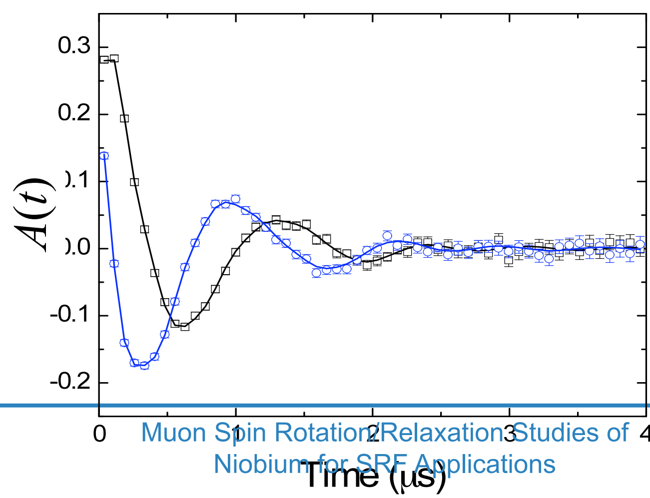

Fourier transform

TF-muSR on cutout samples

- **DC field perpendicular to sample, T=2.3K (and measurements at 4.5K up to 8K), full scan in field 0-270mT**

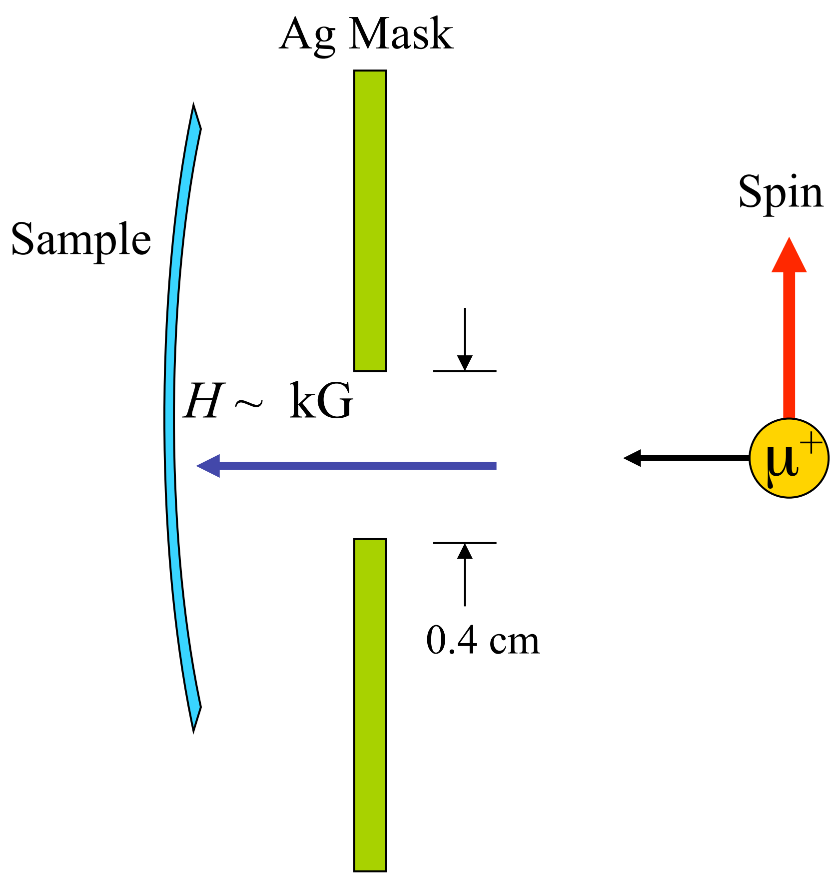

Muon stopping depth ~300μm

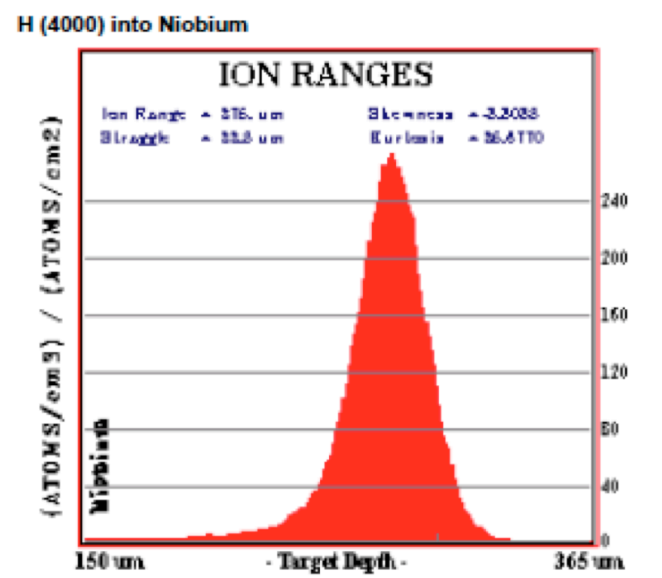

Zero Field muSR

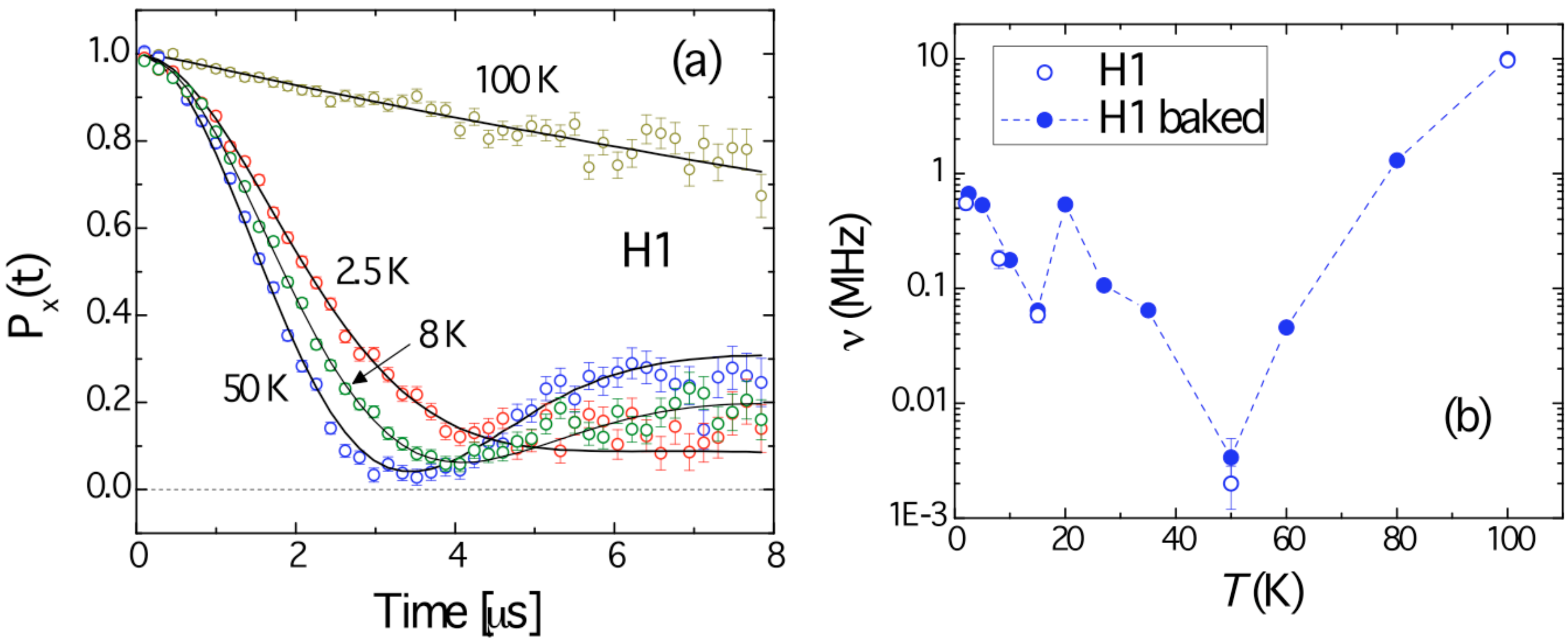

(a) Representative ZF-μSR spectra of sample H1 at different temperatures.
(b) Temperature dependence of the muon hop rate in sample H1 before and after baking.

Results consistent with what observed in μSR experiments on nitrogen doped Nb

Asymmetry signals, 30 and 120mT, 2.3K

C1- cold spot large grain cutout, **H1 – hot spot large grain cutout**

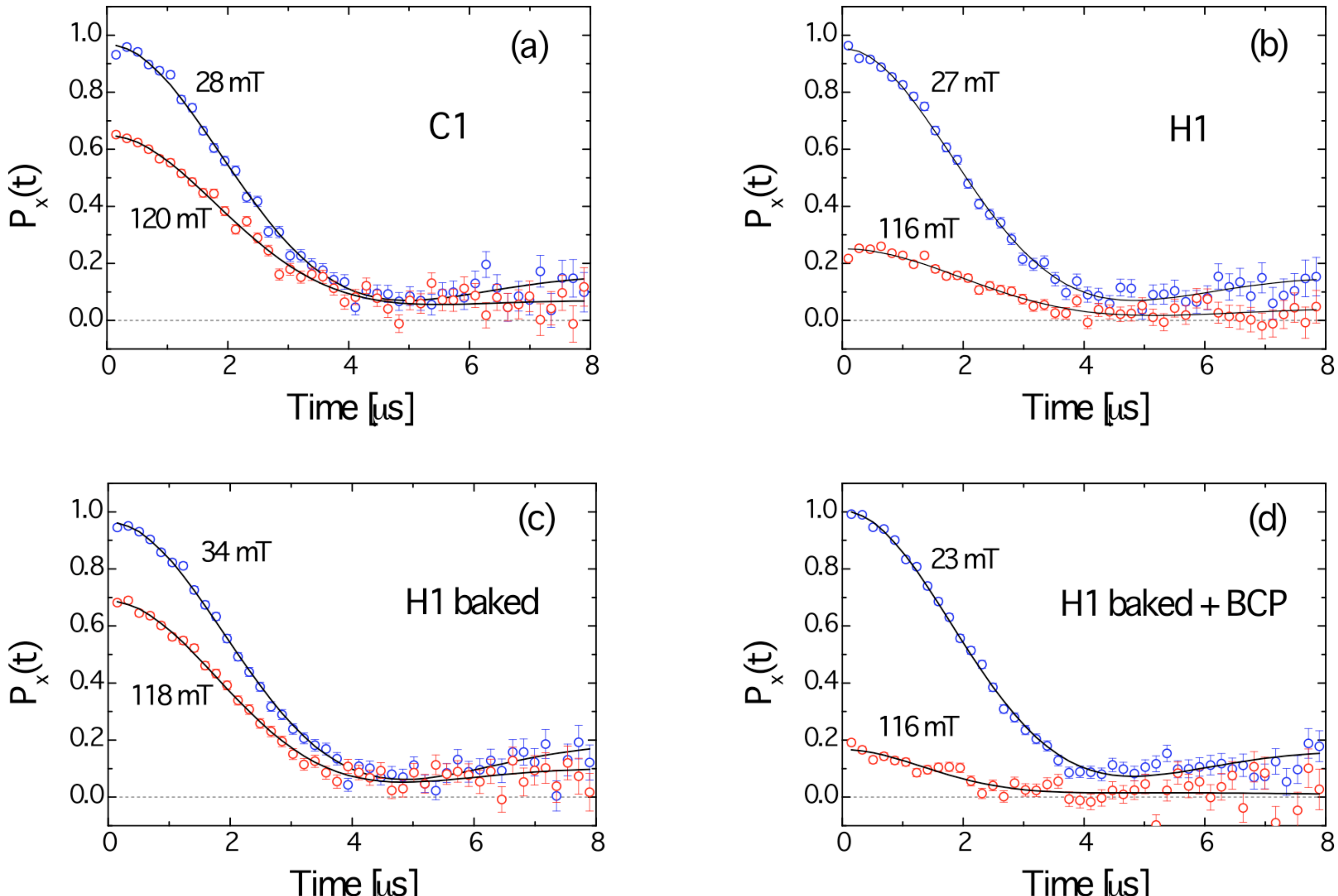

H1 after 48 hours UHV 120C baking

H1 after 48 hours UHV 120C baking plus 5μm BCP

Fast Fourier Transform: internal field distribution

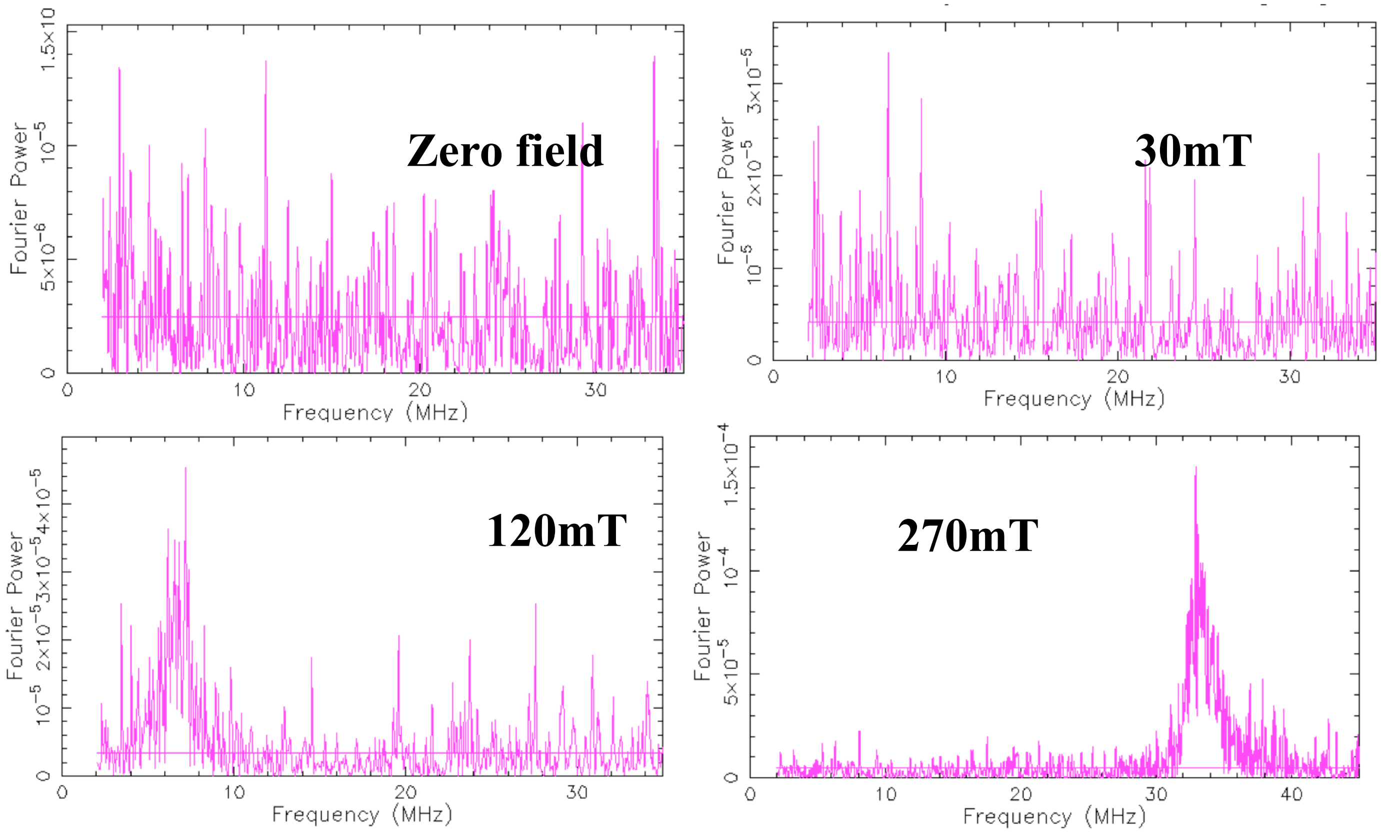

Fast Fourier transforms for sample H1 at 2.3K and respectively field levels: zero, 30mT, 120mT (peak of flux appearing at ~50mT), 270mT (peak of flux ~260mT)
→ Suggests an **inhomogeneous** surface with **preferential sites for flux entry**

Volume fraction of sample NOT containing flux

- The part of the asymmetry signal corresponding to the muons which do not see field in the sample is fitted to a dynamic Gaussian zero-field Kubo-Toyabe
- The fraction corresponding to the muons that see field is assumed to relax fast.

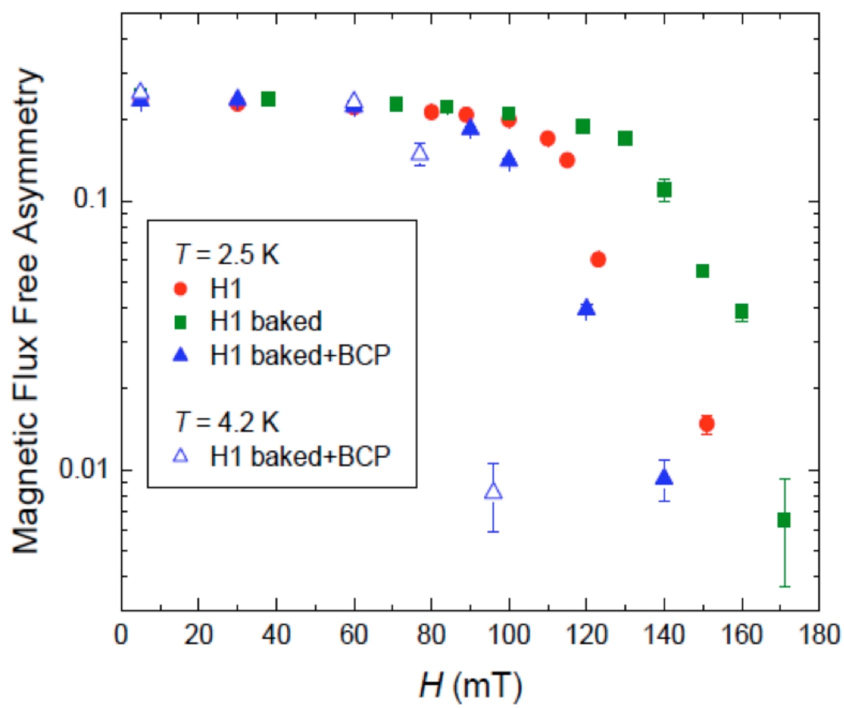

Strong correlation fraction of sample containing flux vs RF cavity performance

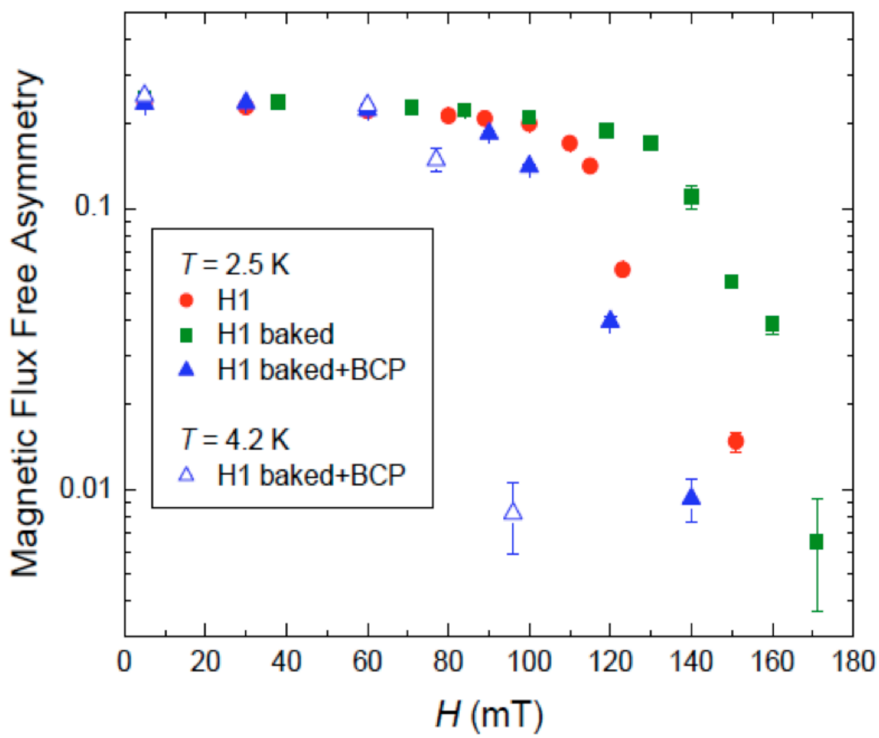

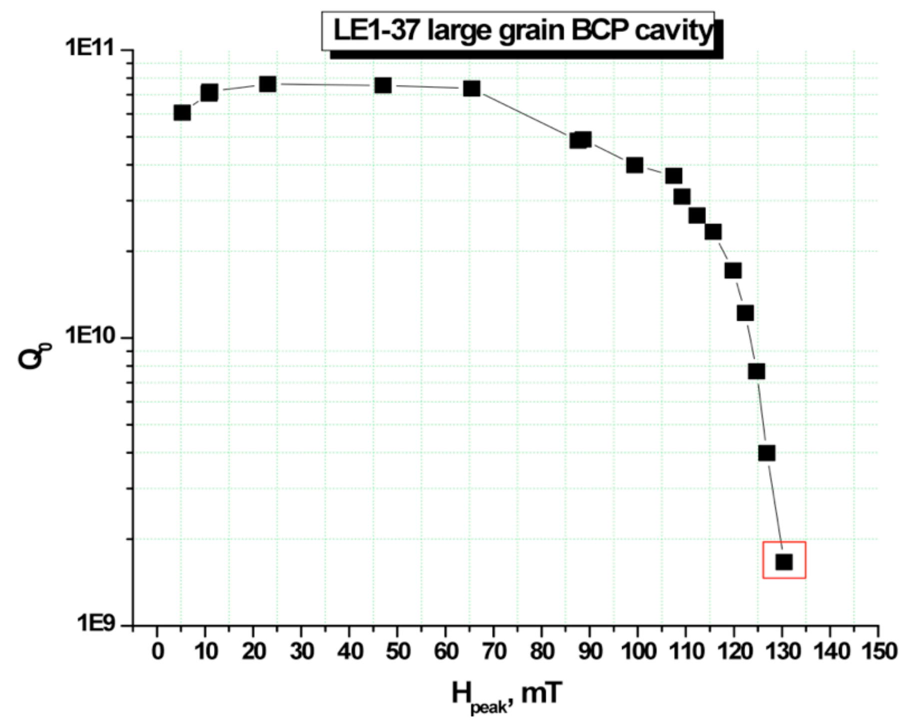

•Onset of flux entry measured with muSR strongly correlates with onset of RF HF losses as for thermometry characterization
•Measurements consistent among all 6 samples tested

Hot vs Cold sample

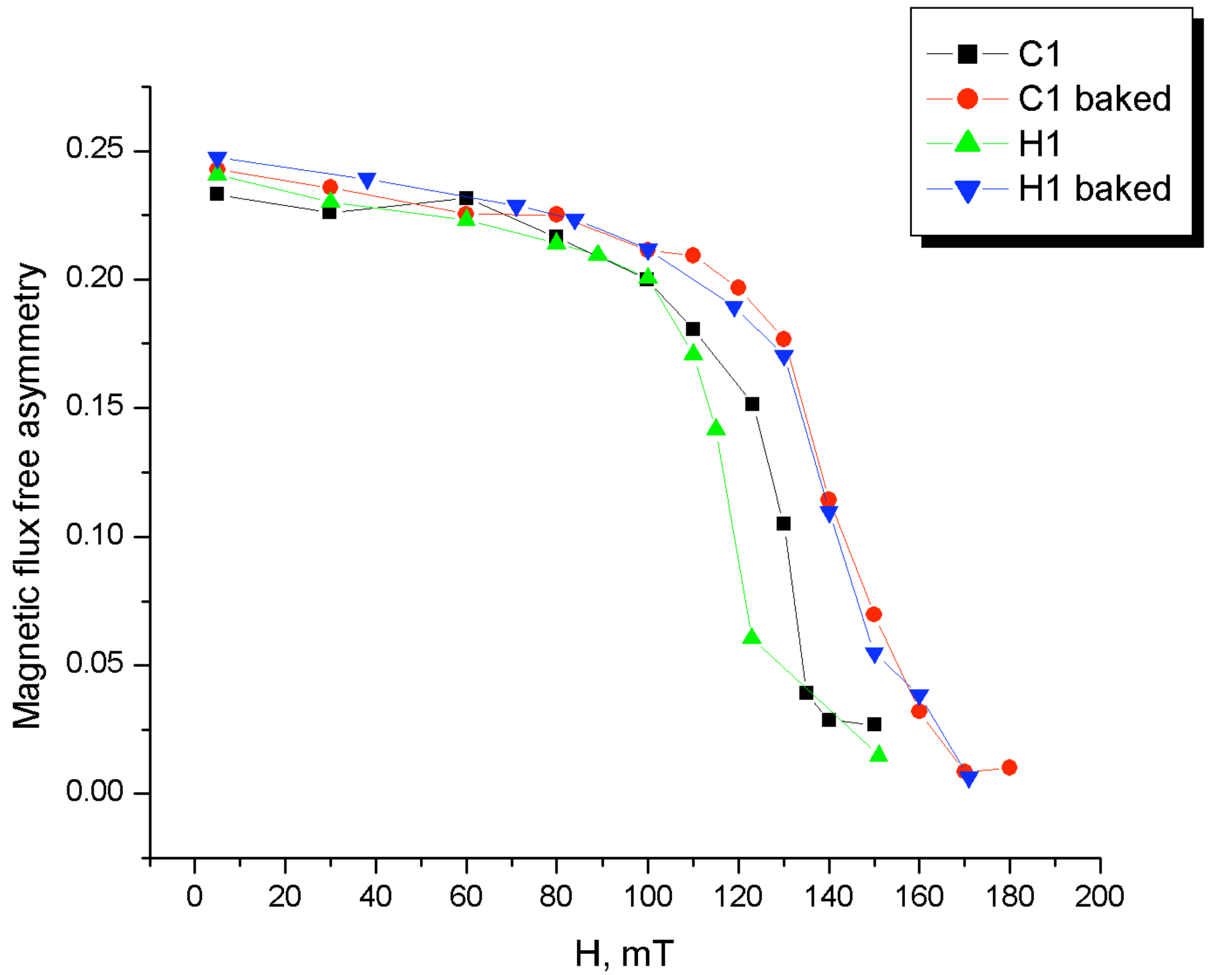

In conclusion

- Muon spin rotation used for SRF applications for the first time
- Experiment results strongly suggest early magnetic flux entry at ‘weaker spots’ as losses mechanism in SRF Nb cavities
- Invaluable tool for studying superconducting parameters
- Field dependent losses can be studied designing experiments with cavities, however it’s vital to gain an understanding of the ‘microscopic’ world
- It’s vital to keep working in close contact with the condensed matter world

Future direction

- First establish **baseline**: study **ultrapure Nb** single crystal (field of entry, superconducting parameters)
- Understand **which step of Nb processing for cavities causes early flux entry** → systematic study of field of entry for niobium with different treatments, degree of cold work, RRR…
- **Q_0 and medium field losses** studies: design apparatus for parallel field measurements
- Study **quench** spots
- **Thin films and multilayer**: accurate tool for field of entry
- Beamtime already approved for these studies, to be scheduled in fall
- LEM for penetration depth and role of hydrogen in surface

Thanks for your attention!

Back up slides

Thermometry characterization of losses

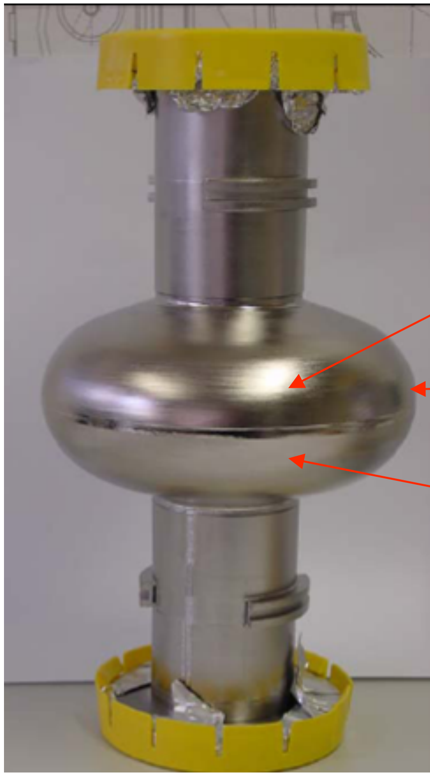

Fine grain

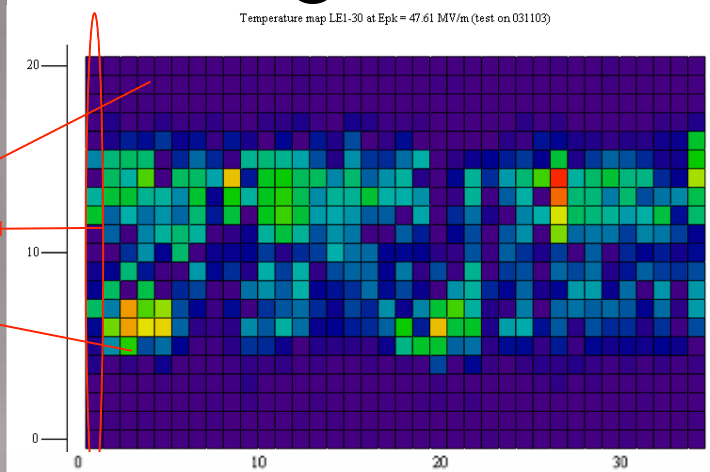

Large grain

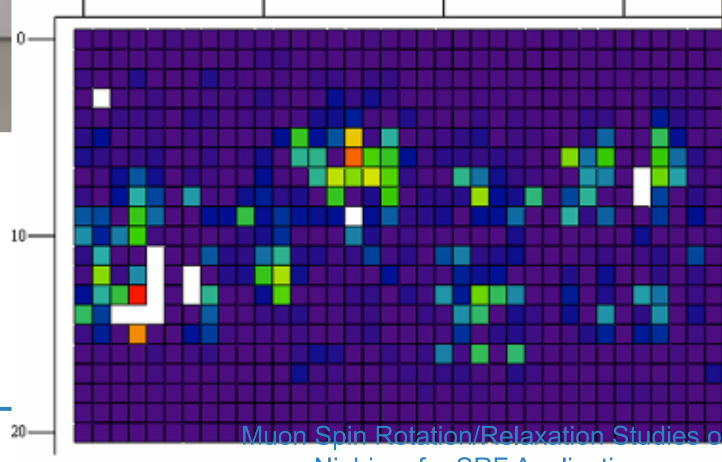

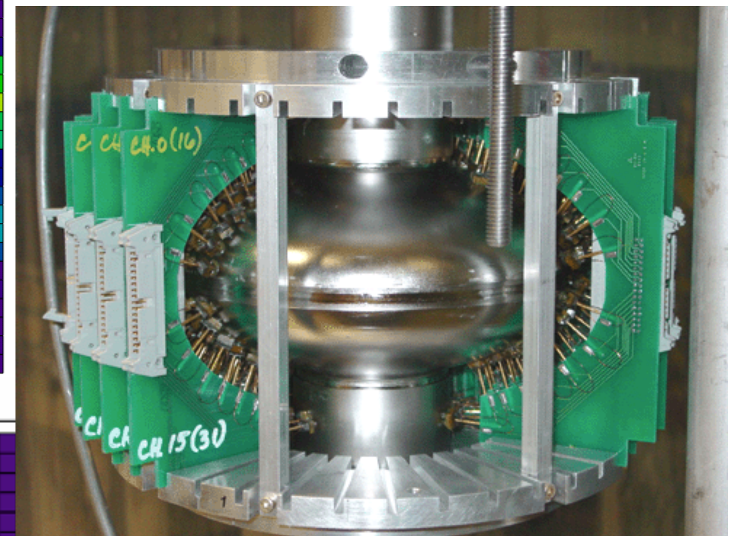

Example of T-map system, G.Ciovati Ph.D. thesis

Thermometry maps, courtesy of Cornell

Brandt – demagnetization

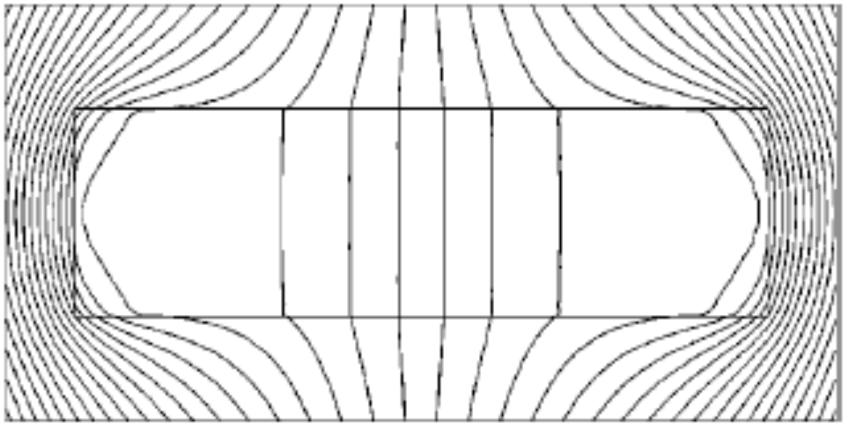

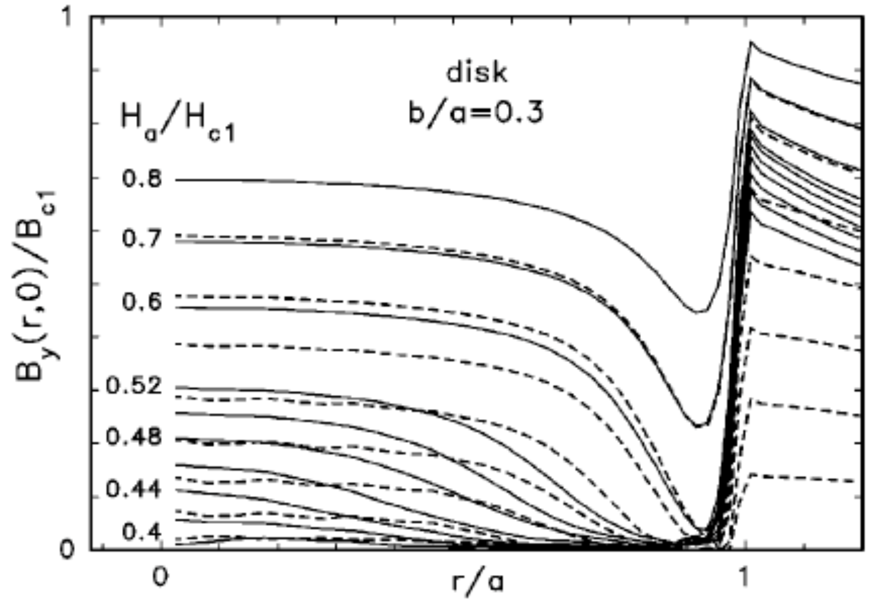

$$H_{en}^{strip}/H_{c1} = \tanh\sqrt{0.36b/a},$$

$$H_{en}^{disk}/H_{c1} = \tanh\sqrt{0.67b/a}.$$

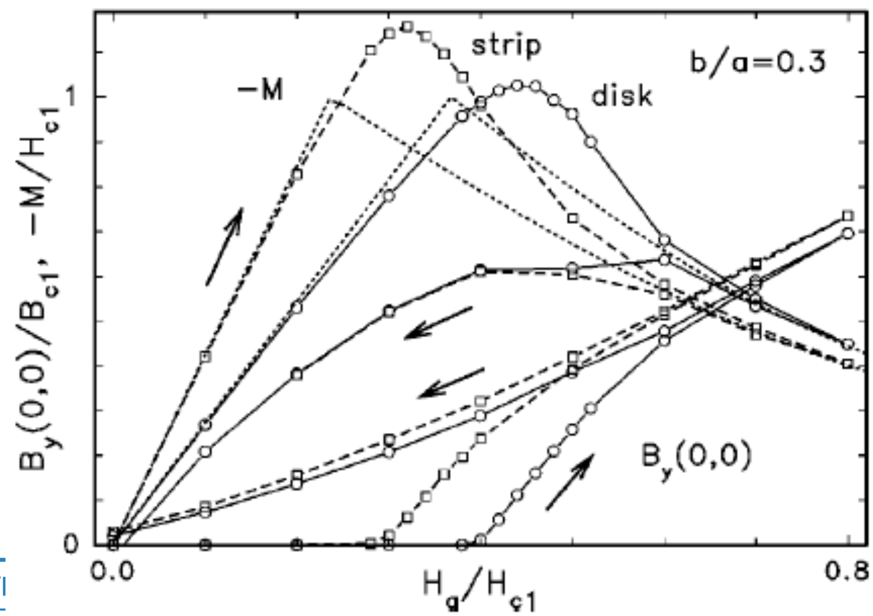

Ernst Helmut Brandt

Irreversible magnetization of pin-free type-II superconductors

PHYSICAL REVIEW B VOLUME 60, NUMBER 17

RF characterization of samples studied (A.Romanenko)

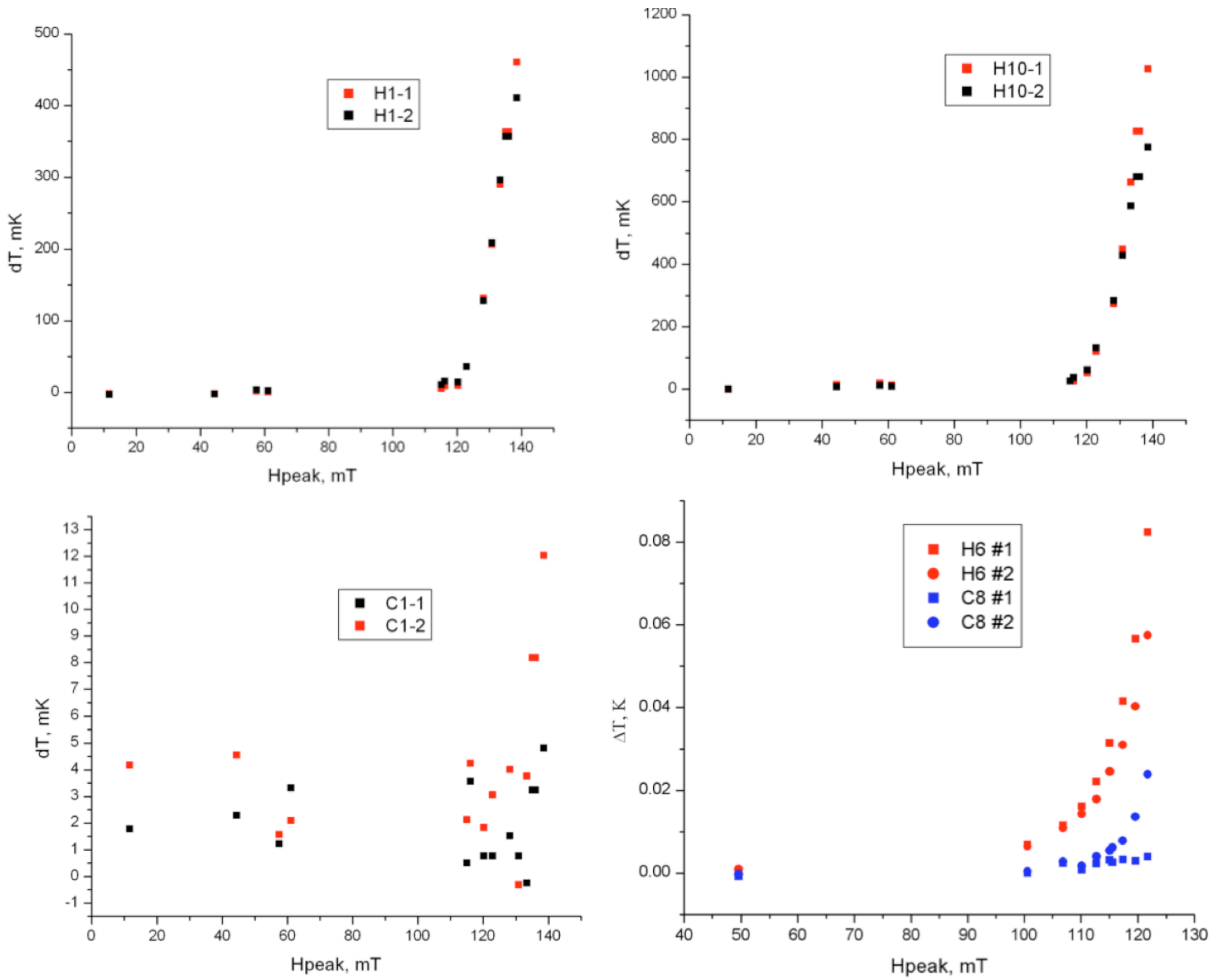

Center vs Annular mask

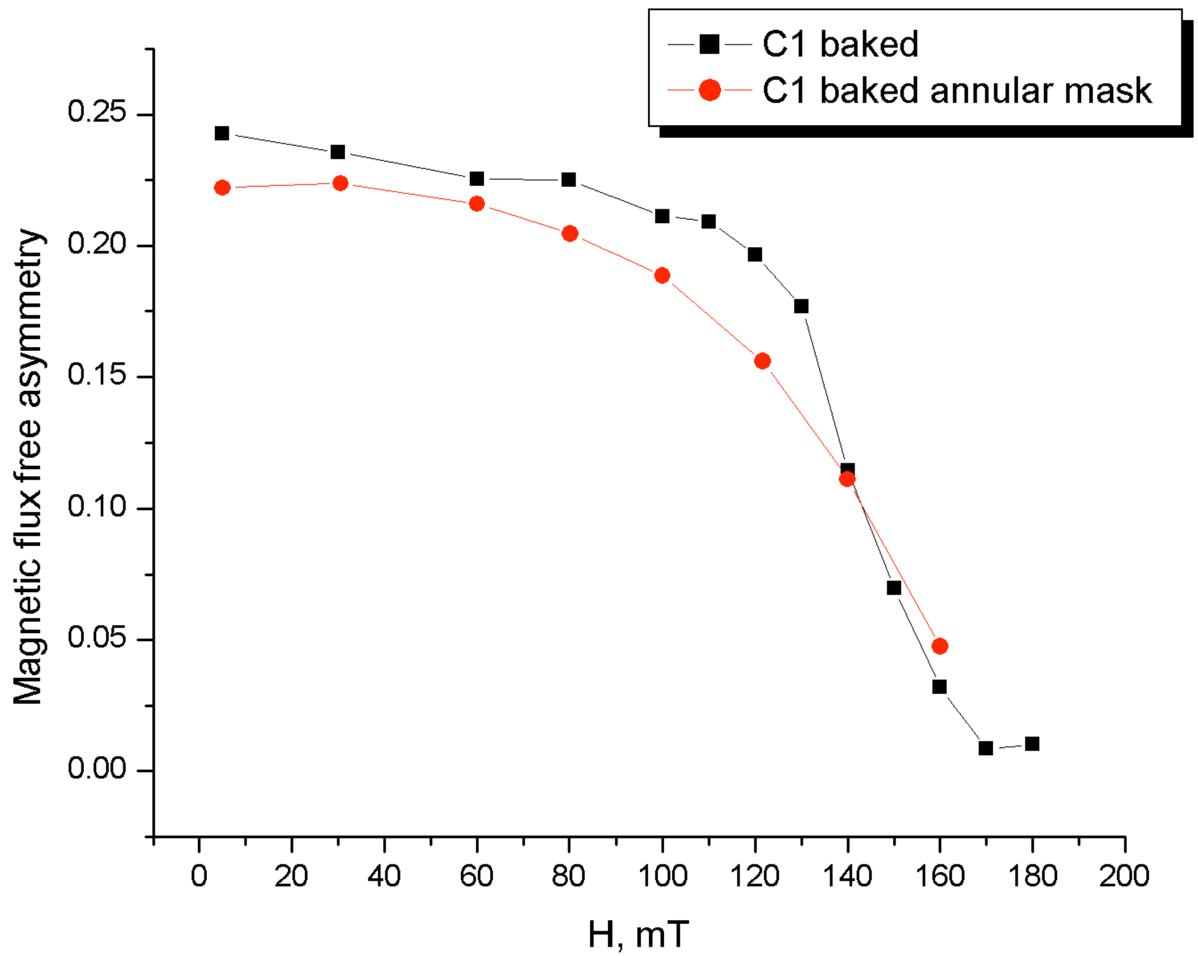

All samples results

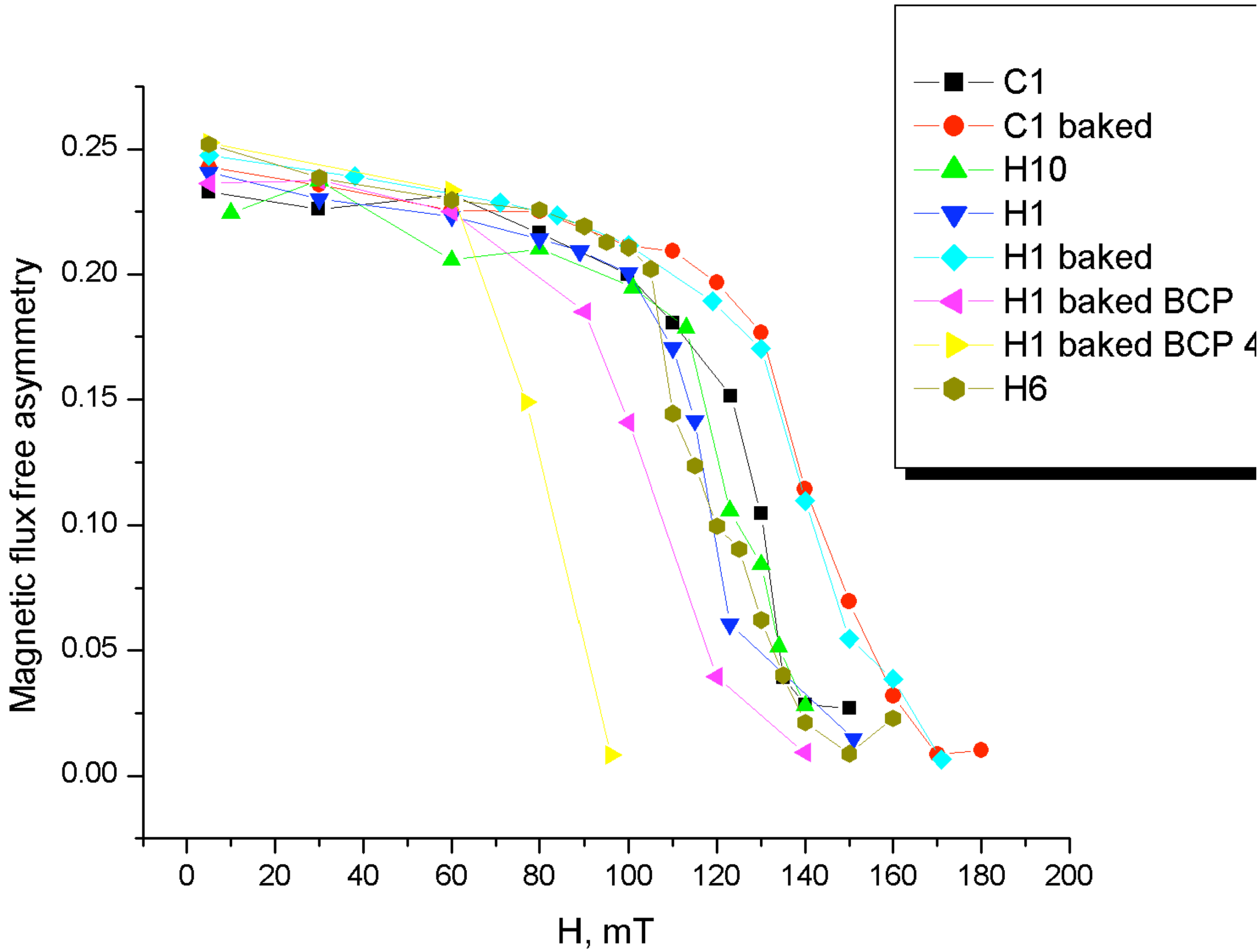

Upper critical field measurement

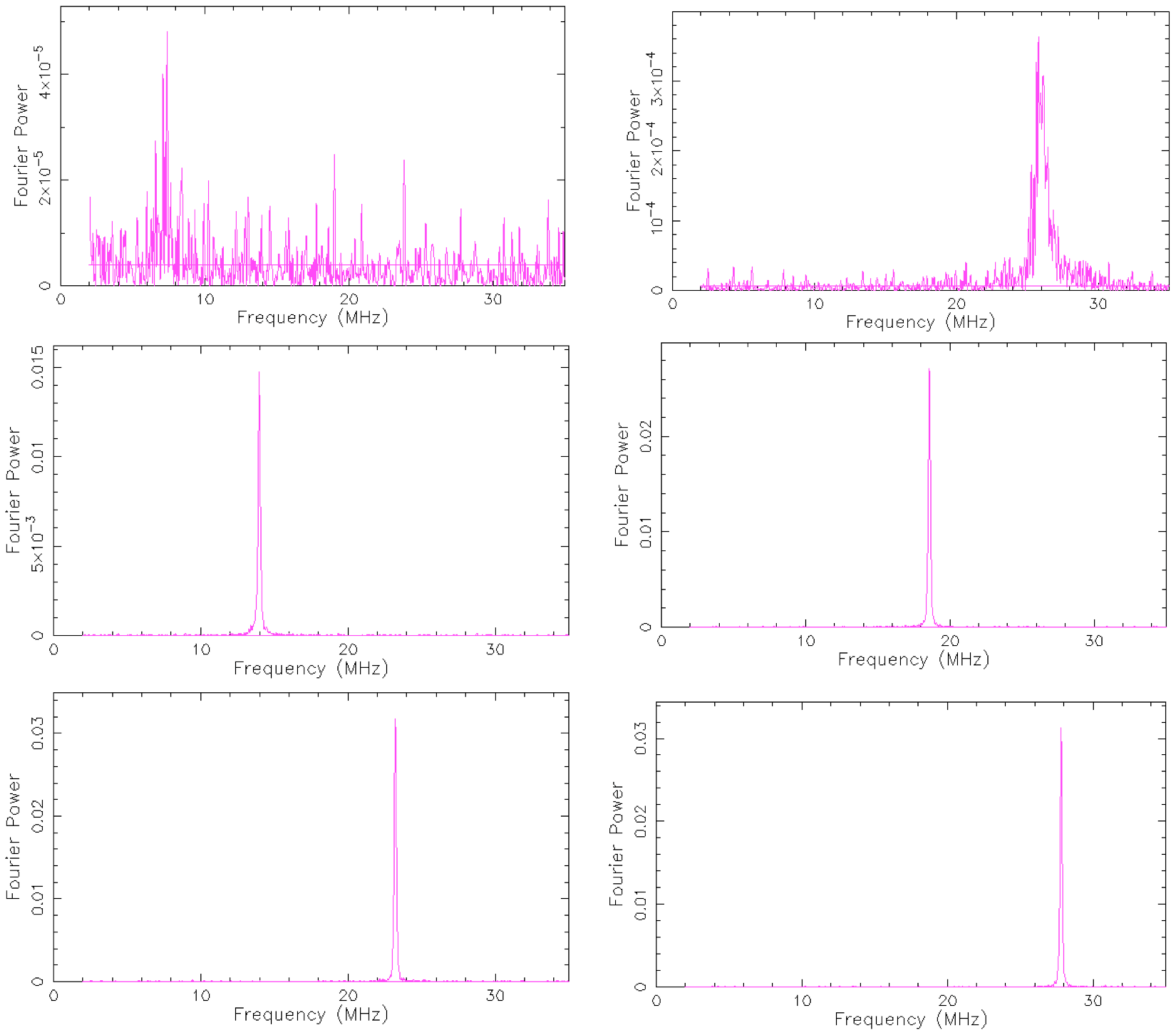

FFTs for sample H10 respectively for temperature and fields: (2.3K, 130mT), (4.5K, 200mT), (7.5K, 100mT), (7.5K, 140mT), (7.5K, 170mT), (7.5K, 200mT)

Coexistence of different 'superconducting' regions?

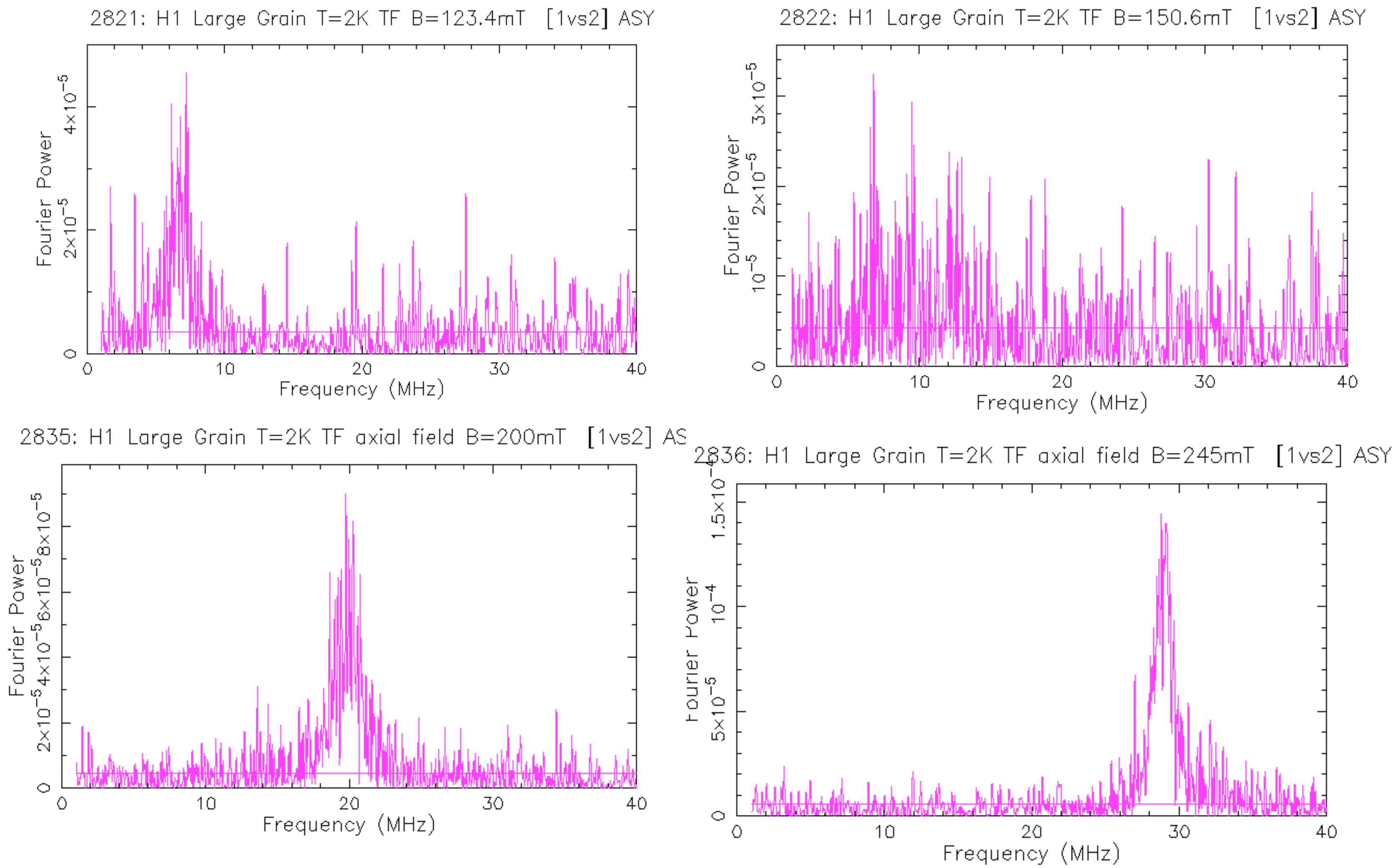

Coexistence of different 'superconducting' regions?

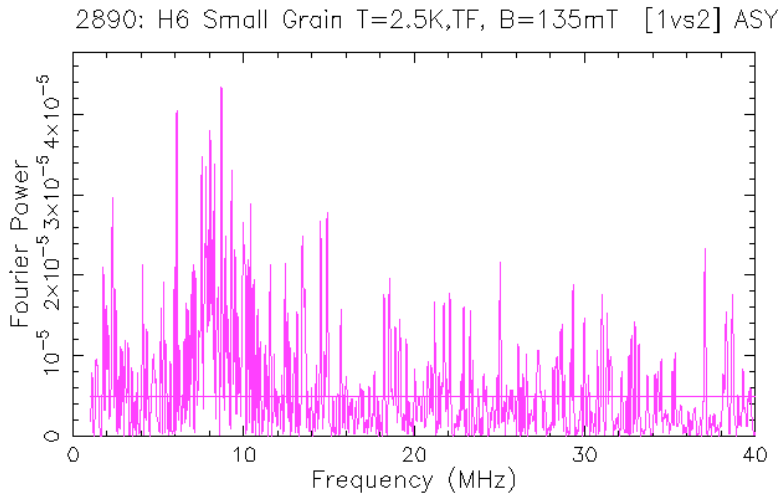

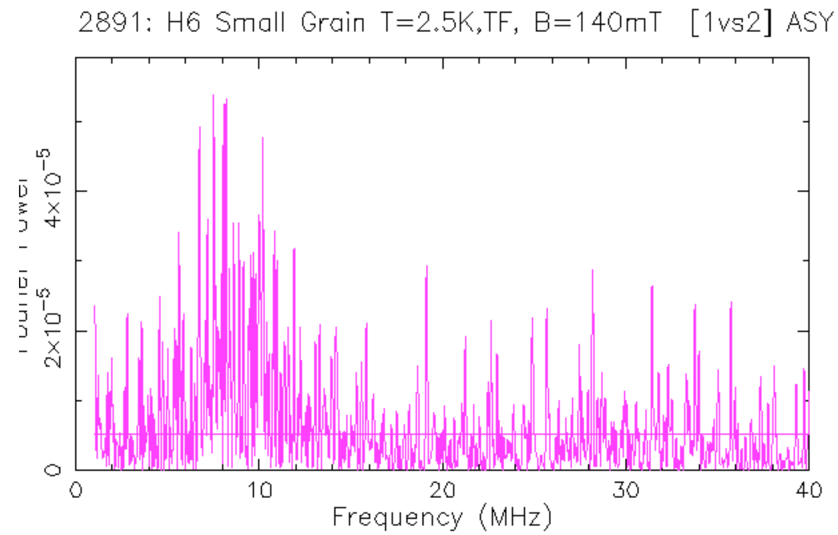

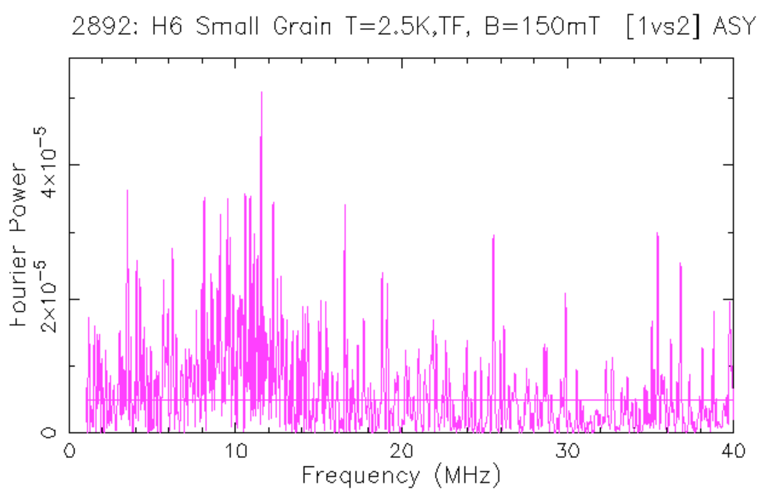

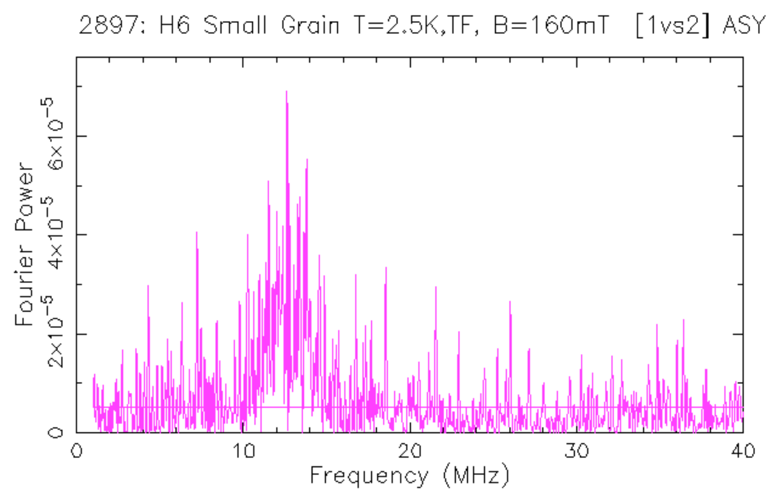

Nuclear Dipolar Relaxation

Nuclei with electric quadrupole moments (such as Cu and Y in $YBa_2Cu_3O_{6+x}$) exert an effective dipolar field B_{dip} on the μ^+. The static (in the μ^+SR time window) internal fields are Gaussian distributed in their values and randomly oriented

$$n(B_i) = \frac{1}{\sqrt{2\pi}} \frac{\gamma_\mu}{\Delta} \exp\left(-\frac{1}{2} \frac{\gamma_\mu^2 B_i^2}{\Delta^2} \right) \qquad (i = x, y, z)$$

where Δ^2/γ_μ^2 is the second moment of the field distribution

The corresponding μ^+ spin relaxation function is known as the ***Kubo-Toyabe function***

$$G_z(t) = \frac{1}{3} + \frac{2}{3}\left(1 - \Delta^2 t^2\right)\exp\left(-\frac{1}{2} \Delta^2 t^2 \right)$$

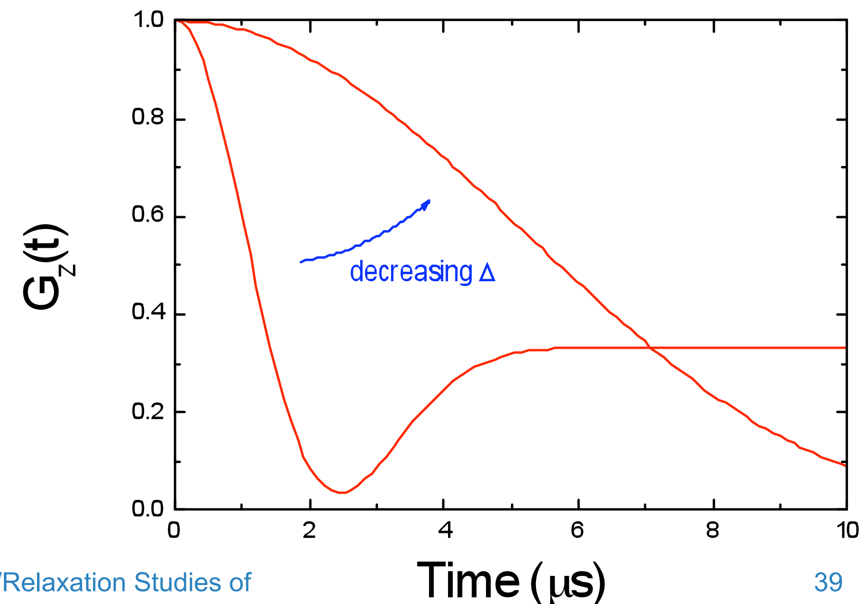

“Effective” Magnetic Penetration Depth: Magnetic Field Dependence

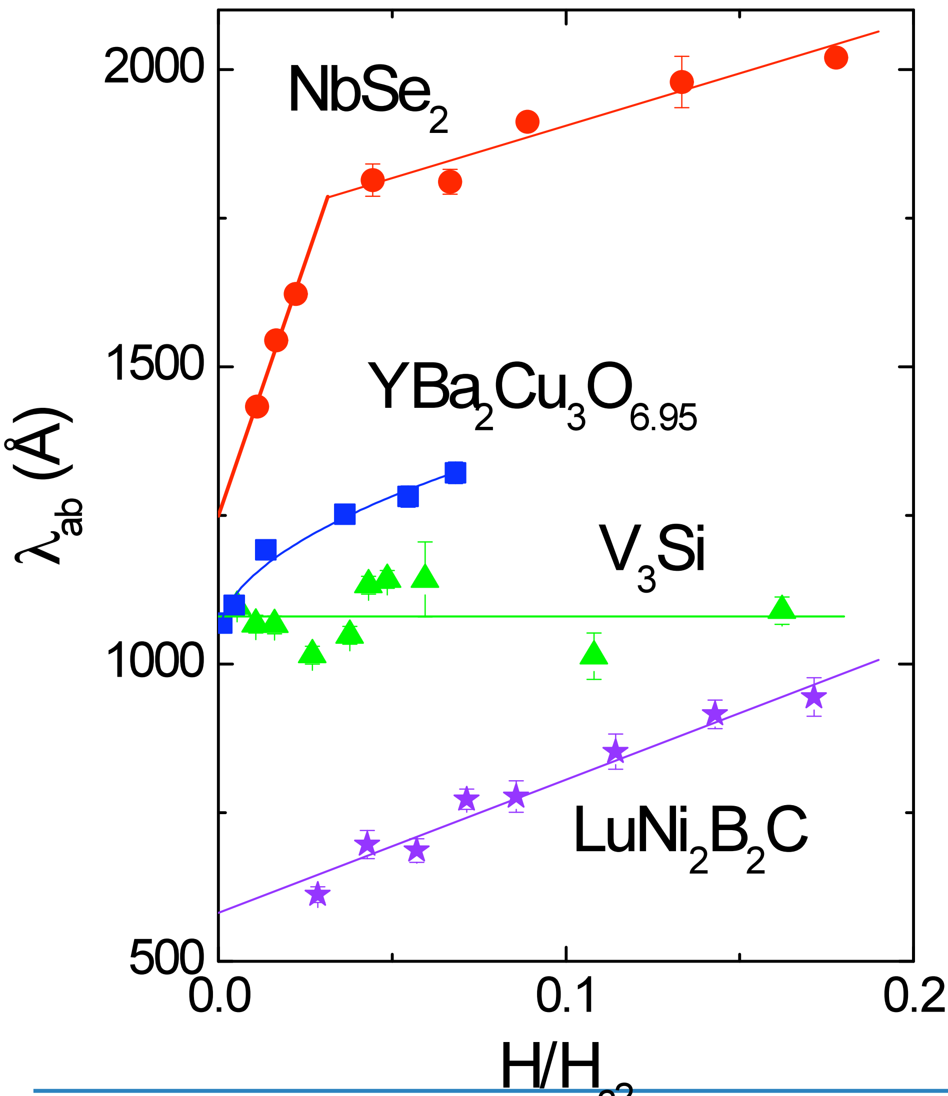

- V_3Si fully gapped
- $LuNi_2B_2C$ anisotropic gap
- $YBa_2Cu_3O_{6.95}$ $d_{x^2-y^2}$-wave gap
- $NbSe_2$ multiband

JES, Rep. Prog. Phys. **70**, 1717 (2007)

Choice of Niobium

- High critical temperature
- High critical field
- Low surface resistance

$$R_S = \frac{A}{T}.\sigma_n.\omega^2.\lambda^3.e^{-B.T_c/T} + R_{\text{residual}}$$

  - Small penetration depth
  - Large coherence length
- Mechanical properties, cost, availability

Material	T_c (K)	λ (nm)	ξ_0 (nm)
Pb	7.2	39	83-92
TYPE I ↑			
TYPE II ↓			
Nb	9.2	32-44	30-60
$Nb_{0.6}Ti_{0.4}$	9.8	250-320	4
NbN	15-17	200-350	3-5
Nb_3Sn	18	110-170	3-6
YBCO	94	140	0.2-1.5

Regime	H_c	H_{c2}	j_c	R_s	T_c	ξ	λ	Material
DC	-	large	large	-	high	small (pinning is needed)	large (bulk current)	NbTi Nb_3Sn
RF	large	-	-	small	high (R_s depends on T/T_c)	large (to give little sensitivity to structure defects)	small $R_s \propto \lambda^3$	Nb Nb(Ti)N ? Nb_3Sn? YBCO?
	Primary requirements					Consequences		

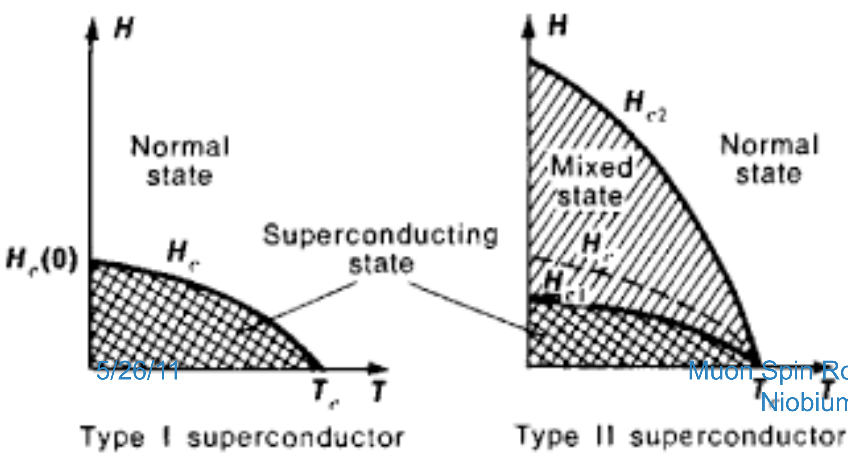

Detection in a cryogenic environment

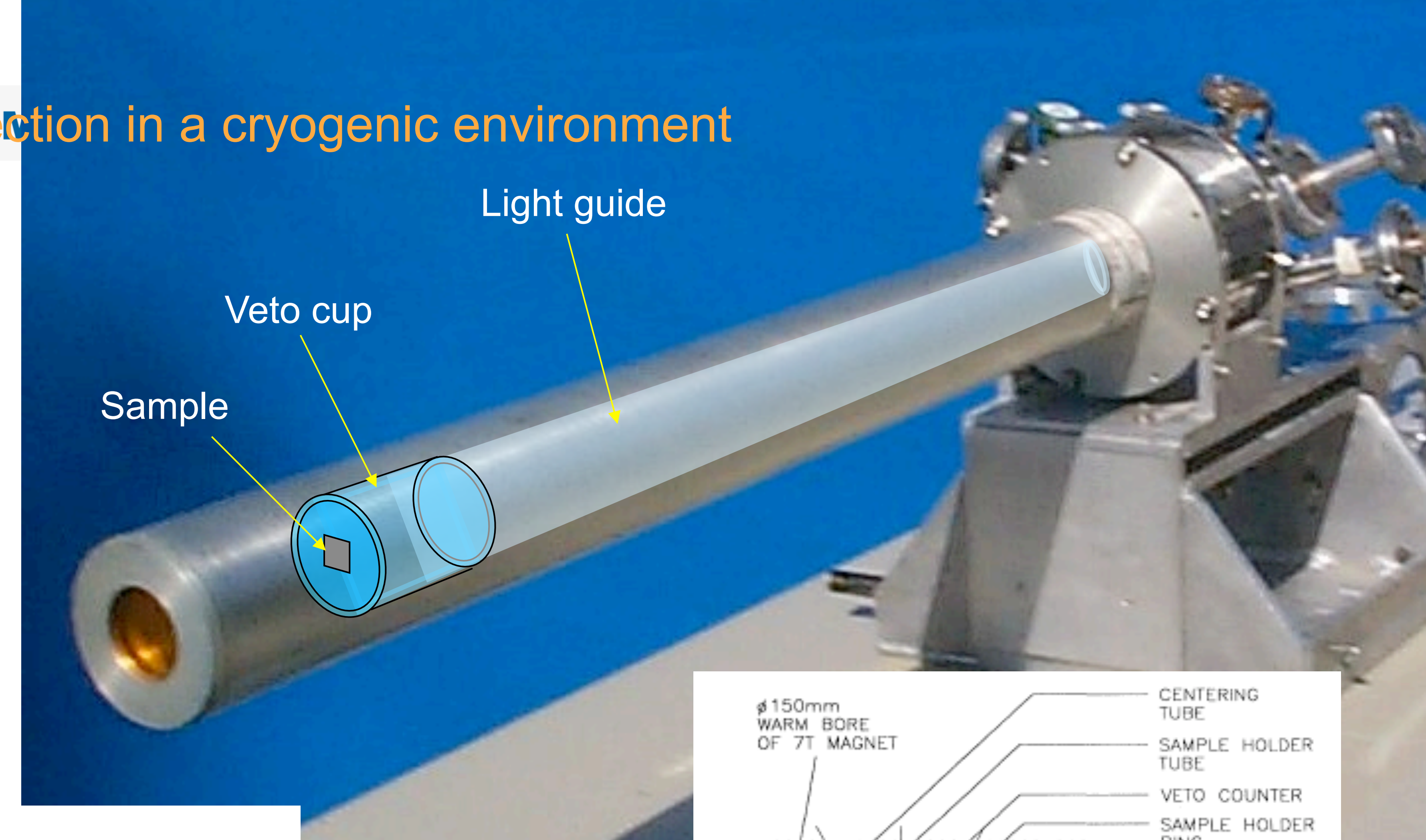

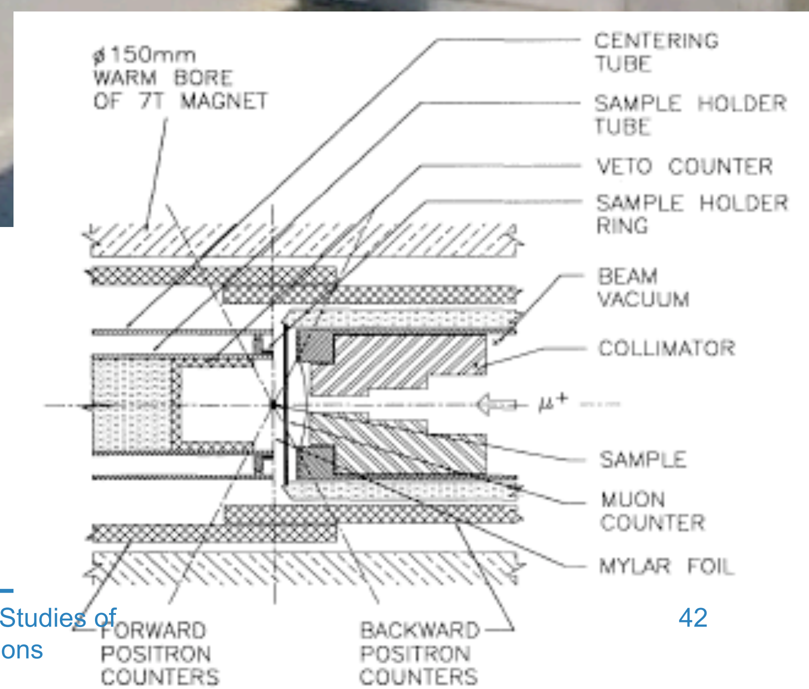

Mechanism to prove right or wrong: HFQS caused by flux entry?

- Measure Hp, Hc2, Tc in samples: S1 (pristine as received by vendor), S2 (BCP+10h 600C), S3 (S2 plus 10h 120C)
- But these samples are different from what final Nb is in our cavities
- And they lack RF characterization

Table 1. H_P and H_{C2} at 2 K and T_C of various samples of Nb.

Sample	T_C (K)	H_P (Oe)	H_{C2} (Oe)
Nb S_1-LG	9.2	1800	6500
Nb S_2-LG	9.05	1050	3700
Nb S_3-LG	9.08	1250	3800
Nb S_1-FG	9.26	1600	7500
Nb S_2-FG	9.05	950	3800
Nb S_3-FG	9.08	1100	4000

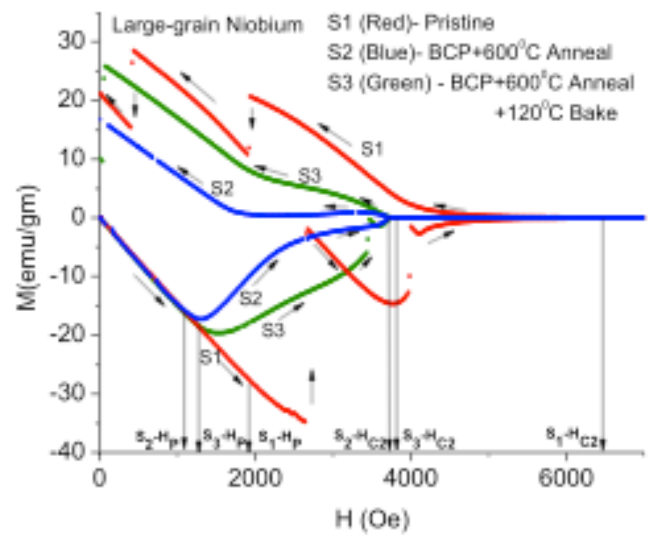

Figure 5. Isothermal *M–H* plots of LG-Nb samples starting from the zero field cooled state at 2 K.

Roy, Myneni et Sahni, Supercond. Sci. Technol. **22 (2009)** 105014 (6pp)